



Assignment for PMIM-702 Dissertation

| | |
|---|---|
| Module number: | PMIM-702 |
| Module name: | Health Data Dissertation |
| Title of assignment: | <i>Publication Ready Paper</i> |
| Student ID number: | 2372776 |
| Word count: | 4,993 |
| Declaration: | I understand the following conditions which apply throughout this course: <ol style="list-style-type: none">1. I confirm that I am the sole author of this work.2. I understand that proof reading by a third party is discouraged, but if used, records should be available as per guidelines.3. I understand the need for academic integrity and that all my submitted work will adhere to its principles.4. I understand that the teaching team will take measures to deter, detect and report any academic misconduct.5. I agree to my work being submitted to the TurnItIn academic database.6. I understand the importance of assignment deadlines and the need to seek help in good time where personal circumstances interrupt my work. |
| Please copy and paste this declaration onto the front of the submission. | |

**A Low-Cost 2D Marker-Based Smartphone System for Distinguishing Normal and
Simulated Pathological Gait**

Michael Leighton

Candidate number

2372776

MSc Health Data Science

Supervisor: Dr. Owen Bodger

Submission date: February 17, 2025



**Swansea University
Prifysgol Abertawe**

ACKNOWLEDGEMENTS

I want to thank Dr. Owen Bodger for his continued support and guidance throughout this project.

Abstract

Quantitative gait analysis plays a crucial role in diagnosing and monitoring neurological and musculoskeletal conditions, yet access remains limited by the high cost and complexity of traditional motion capture systems. This study involved the development of a low-cost de novo smartphone-based software system to evaluate whether it could detect characteristic differences between normal and simulated walking patterns across multiple speeds.

Four healthy adults (ages 22-26) performed three gait conditions (normal, simulated limping, and simulated Parkinsonian) at three walking speeds (2.5, 4, 5.5 km/h) on a treadmill. Kinematic data were captured using an iPhone 7 (60 fps) and four markers tracking hip, knee, ankle, and foot positions in the sagittal plane. Marker trajectories were processed using custom algorithms to calculate joint angles and spatiotemporal parameters.

The system successfully identified distinctive kinematic signatures across gait conditions. Parkinsonian gait showed significantly reduced knee ROM (36.6° vs 57.5° at 2.5 km/h) and characteristic spatiotemporal adaptations, including shortened stride length (31% reduction at 4 km/h) with compensatory increased cadence (92.6 vs 65.4 steps/min). Movement variability analysis demonstrated strong measurement consistency for normal gait, with higher variability in limping and Parkinsonian gait, reflecting individual differences in gait simulation rather than measurement error.

This marker-based smartphone system effectively distinguished between normal and simulated pathological gait patterns by detecting characteristic kinematic and spatiotemporal parameters. While the small sample size and use of simulated gaits necessitate further validation with clinical populations, this approach offers a promising low-cost alternative for quantitative pathological gait assessment in resource-limited settings.

Key Terms

antalginic gait; cadence; freezing of gait (FoG); gait analysis; heel strike (HS); kinematics; Linear Discriminant Analysis (LDA); marker-based tracking; neurological disorders; Parkinson's disease (PD); range of motion (ROM); smartphone-based motion capture; stance phase; stride length; swing phase; toe-off (TO)

TABLE OF CONTENTS

| | |
|---|-----------|
| 1. INTRODUCTION | 6 |
| 1.1 BACKGROUND..... | 6 |
| 1.2 GAP AND OPPORTUNITY..... | 6 |
| 2. METHODS | 7 |
| 2.1 PARTICIPANTS AND STUDY DESIGN | 7 |
| 2.2 EXPERIMENTAL PROTOCOL..... | 8 |
| 2.3 DATA COLLECTION | 8 |
| 2.4 DATA PROCESSING | 8 |
| 2.5 PARAMETER CALCULATION | 9 |
| 2.6 STATISTICAL ANALYSIS..... | 10 |
| 3. RESULTS | 10 |
| 3.1 MARKER TRACKING | 10 |
| 3.2 KINEMATIC ANALYSIS | 12 |
| 3.3 SPATIOTEMPORAL ANALYSIS..... | 14 |
| 3.4 CLASSIFICATION ANALYSIS..... | 17 |
| 4. DISCUSSION..... | 17 |
| 4.1 MAIN FINDINGS..... | 17 |
| 4.2 SYSTEM PERFORMANCE | 19 |
| 4.3 PATHOLOGICAL GAIT CHARACTERISTICS | 19 |
| 4.4 CLINICAL IMPLICATIONS..... | 21 |
| 4.5 LIMITATIONS AND FUTURE DIRECTIONS | 22 |
| 5. CONCLUSION..... | 22 |
| REFERENCES | 23 |
| APPENDIX | 29 |

1. INTRODUCTION

1.1 Background

Gait refers to coordinated movement of the limbs during walking and is a key indicator of neurological and musculoskeletal health. Gait disturbances are often an early sign of neurological conditions (Stolze et al., 2002), including Parkinson's disease (PD), multiple sclerosis (MS), stroke, and age-related disorders (Belda-Lois et al., 2011; Gehlsen et al., 1986; Intzandt et al., 2018; Snijders et al., 2007). Quantifying gait changes helps clinicians diagnose conditions and evaluate treatment effectiveness, and with the ageing population increasing, the demand for accessible gait assessment tools is growing.

Traditional gait analysis methods rely on observational assessment, such as timed walking tests and rating scales (Hobart et al., 2003; Mathias et al., 1986; Tinetti, 1986). While widely accessible, these methods are prone to observer bias and inter-rater variability. Modern objective gait analysis systems use optical motion capture as the gold standard, offering detailed spatiotemporal parameters and joint angles (Cappozzo, 1984). However, these systems cost tens of thousands of pounds and require complex setup, extensive calibration, and specialised training (Hulleck et al., 2022).

Motion capture methods include both marker-based systems, which are highly accurate but require skin-tight clothing and are susceptible to soft tissue artefacts (STA) (Benedetti et al., 2017), and markerless systems, which offer simpler setup but are less precise, particularly with pathological gait patterns (Wang et al., 2025). Smartphone-based methods have emerged as a potential bridge between these approaches and the need for affordable tools. While two-dimensional (2D) video analysis cannot capture out-of-plane movements, sagittal plane assessment effectively evaluates key kinematic parameters in neuropathologies (Andrysek et al., 2007; Fatone & Stine, 2015), though current computer vision approaches still show lower accuracy than marker-based methods (Min et al., 2024; Scataglini et al., 2024). This highlights the need for accessible solutions that balance affordability with robust measurement precision.

1.2 Gap and Opportunity

Despite advances in motion capture and AI-driven markerless tracking, a significant gap remains between the need for quantitative gait analysis and the accessibility of assessment tools. Although smartphone-based marker systems show promise as an accessible solution,

their ability to detect pathological gait patterns requires further validation, particularly in relation to tracking accuracy, stability, and clinical validation (Horsak et al., 2023).

This study involves the development of a low-cost de novo software framework to evaluate whether a 2D smartphone-based marker system can detect and distinguish between normal and simulated pathological gait patterns across different walking speeds. Two distinct gait patterns were selected for testing: Parkinsonian gait (representing reduced movement typical in neurological disorders) and antalgic limping gait (representing asymmetrical movement typical in musculoskeletal adaptations). The contrast between these patterns allows for a more comprehensive assessment of the system's detection capabilities, and as PD is the most studied disease in gait analysis (Sethi et al., 2022), successful testing could promise considerable utility.

This study aims to bridge the gap between quantitative, reliable motion capture and low-cost measurement devices by creating and validating a smartphone-based software system, offering a more accessible alternative for clinical and research use.

2. METHODS

2.1 Participants and Study Design

This proof-of-concept study employed a repeated measures design to evaluate a 2D marker-based smartphone system for gait analysis. Four healthy adults (two female and two male, ages 22-26) performed nine experimental walking tasks each, yielding 371 gait cycles across all conditions. Simulated Parkinsonian gait (characterised by shortened stride length and increased cadence) and antalgic limping (characterised by asymmetrical weight bearing) were selected as test conditions due to their distinct characteristics and reliable simulation potential (Auerbach & Tadi, 2023; Mirelman et al., 2019). Inclusion criteria required healthy adults aged 18-30 years, excluding those with pathological conditions affecting gait.

This study was approved by the Swansea University Medical School Ethics Committee (2025 12449 11641). All participants provided written informed consent. Data collection ensured privacy through standardised clothing and recordings limited to lower extremities. Data were anonymised using ID codes, stored securely, and will be retained for 10 years per institutional policies and then destroyed.

2.2 Experimental Protocol

Participants performed three gait conditions (normal, limping, Parkinsonian) at three walking speeds (2.5, 4, 5.5 km/h) on a treadmill. Each subject performed the tasks for the normal gait condition, starting at 2.5 km/h and ending at 5.5 km/h, before repeating the sequence with limping and Parkinsonian gait. Walking speeds were selected to represent slow, normal, and fast walking based on typical clinical gait analysis protocols. Each 10-second task was preceded by familiarisation and standardised rest periods. 10-second recordings provided sufficient gait cycles for analysis while minimising participant fatigue. For limping gait, participants reduced weight-bearing on the measured limb; for Parkinsonian gait, they adopted a shuffling action with slight flexion in the knees, a shortened stride length and stepping height (Appendix Figure 1). Participants gently held the treadmill support rail to prevent arm-swing occluding markers.

2.3 Data Collection

The recording used an iPhone 7 (60 fps, 1080p) mounted 3 m from the subjects' left sagittal plane at roughly hip height (820 mm) to reduce parallax effects. Participants wore dark skin-tight clothing, and four 40 mm white spherical markers were attached to the greater trochanter, lateral femoral epicondyle, lateral malleolus, and fifth metatarsal head. All wore dark socks with no shoes. Reference to anatomical illustrations of the sagittal plane was used for marker application consistency (García-Pinillos et al., 2016), and markers were not removed or reapplied between tasks. Recordings were conducted under standard indoor lighting conditions.

2.4 Data Processing

This study involved the development of a complete de novo software framework in R (version 2024.04.0), rather than utilising existing motion capture systems. The analysis pipeline consisted of three main stages: 1) individual video processing for marker detection; 2) subject-level analysis for kinematic and spatiotemporal parameters; and 3) combined analysis across all subjects (Appendix Figure 2). Using the 'av' package (Ooms, 2023), video data were processed to extract individual frames as JPEG images while maintaining original video quality and aspect ratio (16:9). Frames underwent grayscale conversion, intensity standardisation, and noise reduction with a Gaussian blur (radius = 1, sigma = 0.30). The custom-developed marker validation system used five criteria: size, circularity,

brightness, contrast ratio, and anatomical constraints. These parameters were individually optimised for each subject to ensure consistent marker detection.

Marker tracking employed a nearest neighbour algorithm with a maximum distance threshold of 40 pixels between consecutive frames with anatomical position constraints. The tracking algorithm assigned markers based on vertical position and proximity to previous frame positions, with specific adaptations for ankle and foot markers when vertical separation was < 5 pixels. Data were smoothed using a 3-frame rolling mean filter, with outlier removal. The choice of a 3-frame rolling mean filter was based on effectiveness in smoothing minor fluctuations while preserving key gait cycle characteristics.

Quality control measures included automated detection of frames with missing markers, with each frame expected to contain precisely four markers corresponding to the expected anatomical zones. Trajectory analysis quantified marker velocity, acceleration and inter-marker distances. Mean velocity, standard deviation, and outliers (>2 SD from mean) were calculated for each marker. Inter-marker distances were assessed using means, standard deviations, and coefficients of variation (CV) for hip-knee, knee-ankle and ankle-foot segments. Suspicious velocities and inconsistent inter-marker distances were flagged for manual review.

Stance phase detection used a multi-stage algorithm tracking ground contact status of the foot over time. Heel strikes (HS) were identified using three criteria: 1) stable ankle position; 2) passing below a predefined height threshold relative to mean height of the ankle; 3) sudden change in vertical velocity. Toe-off (TO) detection required specific conditions: low vertical velocity in the preceding frame, followed by sustained upward velocity across three consecutive frames, with additional checks to prevent false detections. Both events used condition-specific velocity thresholds optimised for each gait pattern and speed, with duration constraints (8-15 frames) ensuring physiologically plausible stance phases. Detection accuracy was verified by comparing automatically detected HS and TO with manual inspection of video frames.

2.5 Parameter Calculation

Knee and ankle angles were computed using vector calculations between relevant markers, with the knee angle calculated as 180° minus the inverse cosine of the normalised dot product, representing the internal angle between thigh (hip to knee) and shank (knee to ankle) vectors. The ankle angle was computed from the inverse cosine of the normalised dot

product between the shank and foot (ankle to foot) vector. Range of motion (ROM) was calculated as the difference between maximum and minimum angles, with safety checks implemented to ensure valid angle calculations when marker positions were detected.

Spatiotemporal parameters were derived from stance phase identification. Using the detected HS and TO events: 1) stride time was calculated from the time between consecutive HS; 2) stride length was calculated multiplying treadmill speed and measured stride time; and 3) cadence was computed from the number of HS per minute. All parameters included validity checks and threshold optimisation for each subject.

2.6 Statistical Analysis

Analysis used repeated measures ANOVA with condition and speed as within-subject factors, using the R package 'ez' (Lawrence, 2016). The Greenhouse-Geisser correction was applied when sphericity was violated. Post-hoc analyses employed Bonferroni-corrected paired t-tests using the R package 'rstatix' (Kassambara, 2024). Effect sizes were calculated using Cohen's d with the R package 'effectsize' (Ben-Shachar et al., 2020). Between-subject variability was assessed using CV for kinematic and temporal parameters. Significance was set at $p < 0.05$ with 95% confidence intervals.

For automated gait pattern classification, Linear Discriminant Analysis (LDA) was performed on the combined kinematic and spatiotemporal parameters. LDA was selected for its suitability with smaller sample sizes and ability to find linear combinations of features that best separate different classes. All features were standardised prior to analysis. Reliability was assessed using a 4-fold cross-validation, with each fold corresponding to a different subject to ensure independence of training and testing data.

3. RESULTS

3.1 Marker Tracking

Analysis of marker trajectories revealed distinct movement patterns between conditions. Movement trajectory plots demonstrated that normal gait exhibited well-distributed, cyclical patterns with consistent inter-marker spacing and smooth, oval-like trajectories (Figure 1A, Appendix Figures 3–10). In contrast, PD gait showed notably compressed movement patterns with reduced vertical excursion of all markers and smaller inter-marker distances,

suggesting a more flexed posture characteristic of Parkinsonian gait. Limping gait demonstrated a distinctive asymmetry in the anterior-posterior progression of distal markers, with foot and ankle markers showing greater posterior excursion relative to the knee compared to their anterior progression. These patterns became more pronounced with increasing speed in normal gait, while PD gait maintained its restricted movement pattern across all speeds. The density heatmaps further highlighted these differences, with normal gait showing broader, evenly distributed movement patterns (indicated by wider spread of

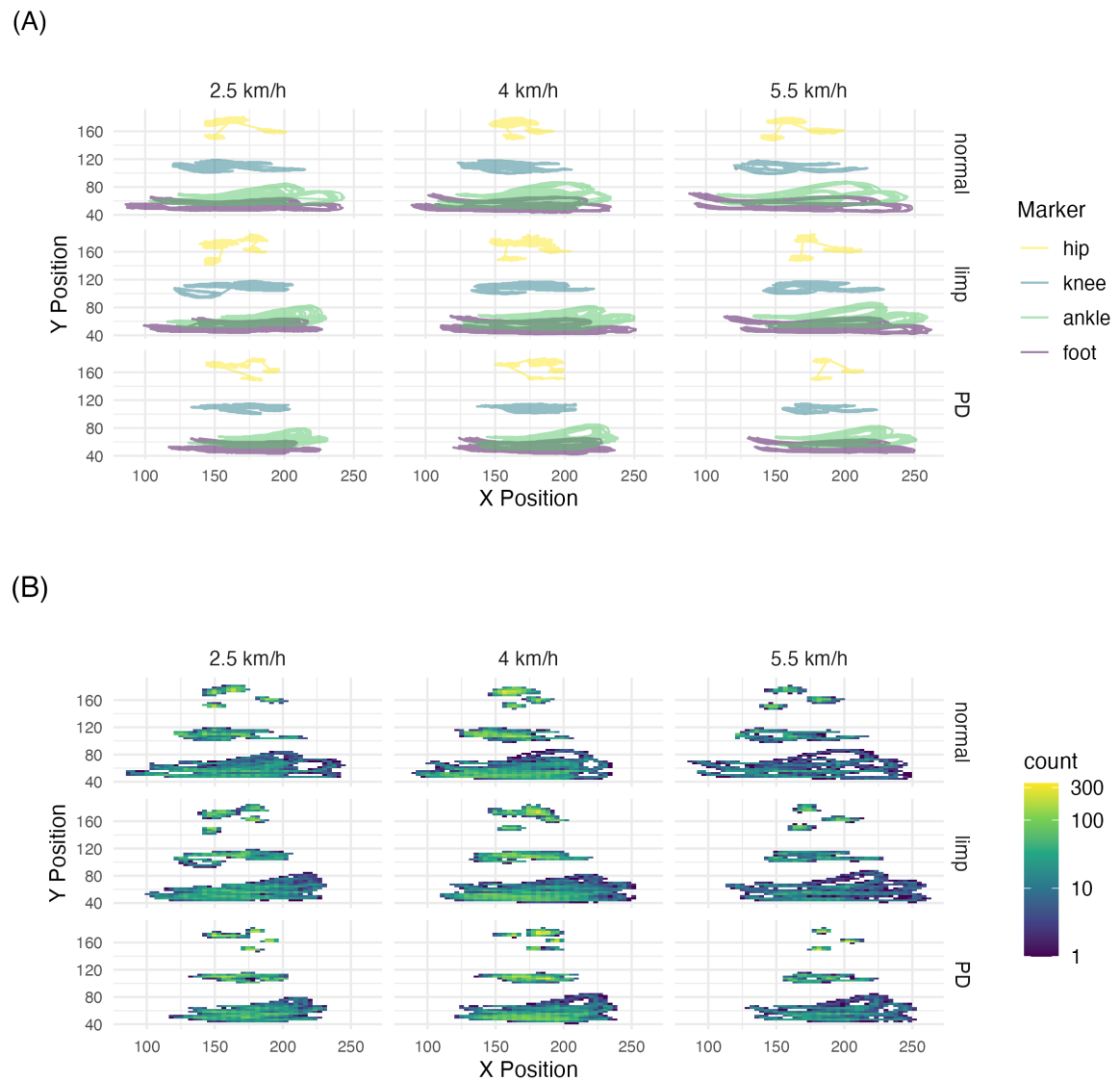


Figure 1. Marker position analysis. Collated data from all four subjects, across ~600 frames per condition/speed. Marker tracking was implemented using a nearest neighbour algorithm. Markers were initially identified by their vertical positions corresponding to anatomical landmarks (hip, knee, ankle, foot). A maximum displacement threshold between consecutive frames prevented marker misidentification during both stance and swing phases. Raw marker position data were smoothed using a 3-frame rolling mean filter to reduce high-frequency noise while preserving the underlying movement patterns. Potential outliers in marker trajectories were identified using statistical thresholds based on deviation from the mean trajectory, and removed from analysis. In frames where marker data were missing but valid markers were detected in adjacent frames, positions were estimated using linear interpolation. (A) Trajectory plot; (B) Heatmap plot.

medium-intensity colours). Conversely, PD gait displayed more concentrated movement patterns (smaller, higher-intensity areas), consistent with reduced movement variability (Figure 1B).

3.2 Kinematic Analysis

The marker system detected clear differences in joint motion patterns between normal and pathological gaits, with knee ROM showing significant main effects for both condition ($F(2,6) = 22.31, p = 0.002$) and speed ($F(2,6) = 26.32, p = 0.001$). Knee ROM was consistently greater in normal gait compared to both simulated conditions, with differences becoming most pronounced at higher speeds (Table 1; Figure 2A – B). At 5.5 km/h, normal gait showed significantly larger knee ROM (64.5°) compared to both limping (50.9°) and PD gait ($51.0^\circ, p < 0.05$), with large effect sizes ($d = 3.25$ and 2.53 respectively). While both normal and PD gaits showed increased ROM with speed, PD gait remained substantially restricted – starting at just 36.6° at 2.5 km/h, nearly 30% lower than normal gait. This restriction persisted across all speeds, highlighting the limited joint excursion typical of Parkinsonian gait. These results indicate that ROM was consistently lower in PD gait across all speeds, while limping gait exhibited intermediate values between normal and PD conditions. The largest differences in knee ROM were observed at 5.5 km/h, where normal gait demonstrated the greatest range of movement.

Ankle motion patterns showed a significant effect for condition ($F(2,6) = 14.46, p = 0.005$) but not speed ($p = 0.150$), with normal gait demonstrating consistently higher ROM

Table 1. Kinematic Parameters Across Walking Speeds and Conditions

| Condition | Speed (km/h) | Knee ROM (°) | | Ankle ROM (°) | |
|-----------|--------------|--------------|-------------|---------------|-------------|
| | | Mean | 95% CI | Mean | 95% CI |
| normal | 2.5 | 57.5 | 49.7 – 65.2 | 42.1 | 30.0 – 54.1 |
| | 4.0 | 61.3 | 56.0 – 66.6 | 43.0 | 31.3 – 54.6 |
| | 5.5 | 64.5 | 59.4 – 69.7 | 45.4 | 29.5 – 61.3 |
| limp | 2.5 | 39.1 | 29.2 – 49.0 | 32.9 | 17.6 – 48.1 |
| | 4.0 | 45.7 | 39.4 – 51.9 | 33.6 | 17.0 – 50.1 |
| | 5.5 | 50.9 | 44.4 – 57.3 | 44.4 | 25.7 – 63.2 |
| PD | 2.5 | 36.6 | 20.7 – 52.5 | 30.5 | 16.1 – 44.8 |
| | 4.0 | 46.2 | 32.1 – 60.3 | 34.0 | 18.5 – 49.6 |
| | 5.5 | 51.0 | 38.9 – 63.1 | 36.6 | 21.9 – 51.4 |

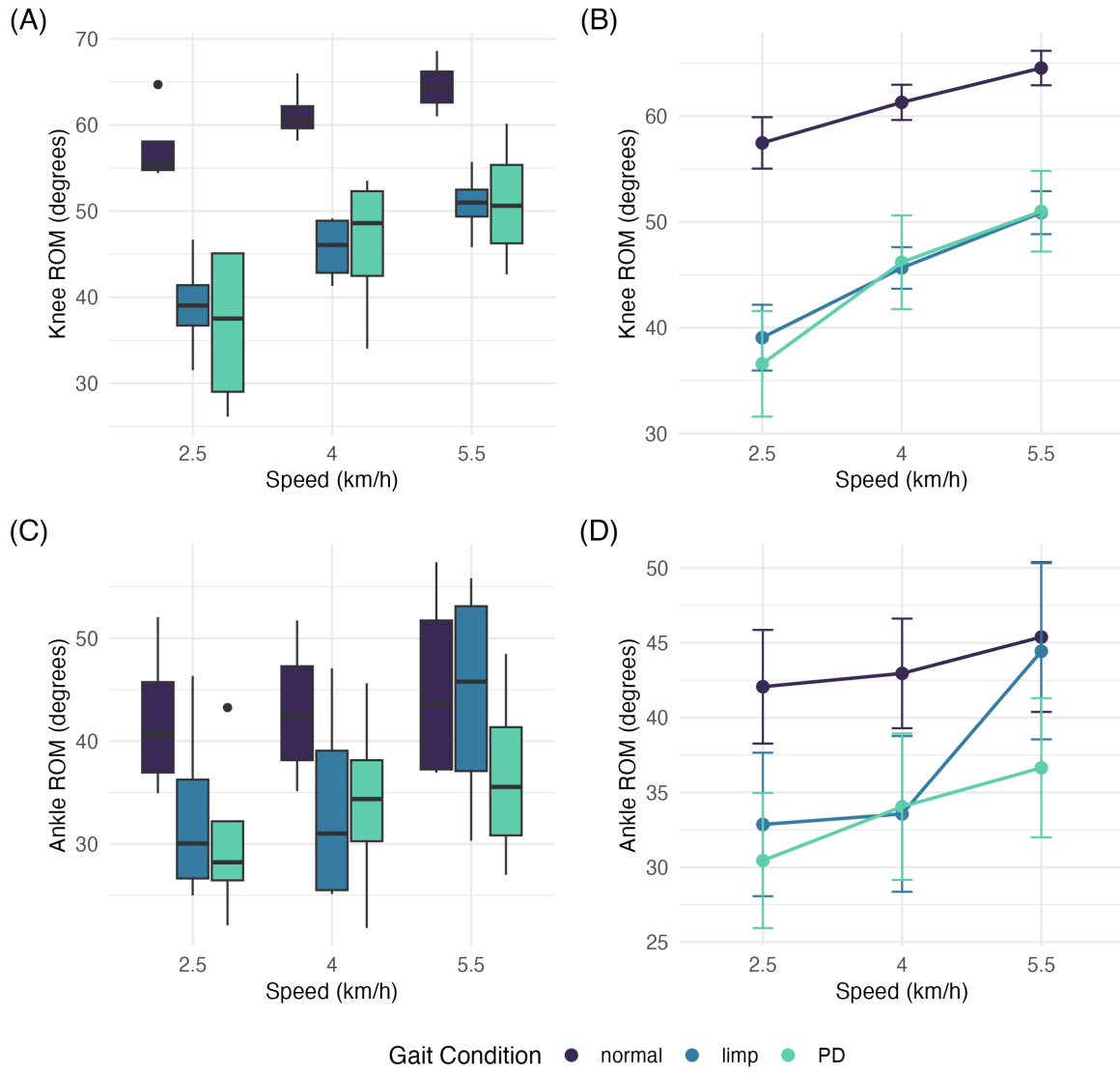


Figure 2. Kinematic differences across gait conditions. The final knee angle was calculated as 180° minus the inverse cosine of the normalised dot product to ensure that the measured values represented the internal (included) joint angle. All angle calculations included magnitude validation to ensure values remained within physiologically plausible ranges. Value clamping was applied to prevent computational artefacts and ensure numerical stability in cases of extreme or missing values. (A) Knee ROM box plot.; (B) Knee ROM line graph; (C) Ankle ROM box plot. (D) Ankle ROM line graph. Error bars: \pm SEM.

compared to PD gait at both 2.5 km/h (42.1° vs 30.5° , $p = 0.038$) and 5.5 km/h (45.4° vs 36.6° , $p = 0.017$) (Figure 2C – D). Although limping gait showed reduced ankle ROM compared to normal walking, these differences did not reach statistical significance at any speed. While participants maintained stable ankle mobility across speeds during normal walking, their simulated Parkinsonian gait showed consistently restricted ankle movement, mirroring the joint rigidity and reduced push-off capacity typical of PD. The lack of a speed-related effect reinforces this notion, indicating that PD gait does not dynamically adapt its ankle movement pattern with increasing speed. In contrast, limping gait showed a trend toward ankle ROM, though the absence of statistically significant differences suggests that

the compensatory mechanisms affecting knee motion may have played a more significant role in adapting to the simulated impairment.

Movement variability showed distinct patterns between conditions (Appendix Table 1). Normal gait demonstrated stable and consistent joint motion patterns (knee ROM CV: 5-8%), indicating a well-regulated and predictable movement pattern. In contrast, pathological gaits displayed greater variability, particularly in ankle movement (CV up to 31%), suggesting a less stable and more irregular motion profile. This increased variability was most pronounced in PD gait at slower speeds, which may reflect difficulties in maintaining rhythmic and coordinated movement, typical with Parkinsonian gait. The greater variability in ankle movement compared to knee movement across all three conditions is likely in part due to inconsistencies in marker tracking due to the larger, faster movements during walking.

3.3 Spatiotemporal Analysis

Timing and distance parameters revealed characteristic patterns for each gait condition, with stance phase showing significant effects for both condition ($F(2,6) = 9.83, p = 0.013$) and speed ($F(2,6) = 17.29, p = 0.003$). While normal and limping gaits maintained similar progressive changes in stance percentages (starting at 71.1% for both, $p > 0.05$), PD gait showed a significantly different pattern, with stance phase reducing from 63.7% at the slowest speed, to 65.8% at normal walking speed, to 54.1% at the highest speed (Table 2,

Table 2. Spatiotemporal Parameters Across Walking Speeds and Conditions

| Condition | Speed (km/h) | Stance (%) | | Stride Length (m) | | Cadence (steps/min) | |
|-----------|-----------------|------------|-------------|-------------------|-------------|---------------------|-------------|
| | | Mean | 95% CI | Mean | 95% CI | Mean | 95% CI |
| normal | 2.5 | 71.1 | 65.7 – 76.6 | 1.01 | 0.92 – 1.10 | 43.5 | 38.7 – 48.3 |
| | 4.0 | 63.9 | 59.7 – 68.2 | 1.25 | 1.12 – 1.39 | 52.5 | 47.7 – 57.3 |
| | 5.5 | 62.9 | 59.7 – 66.1 | 1.44 | 1.26 – 1.62 | 64.5 | 55.4 – 73.6 |
| limp | 2.5 | 71.1 | 62.4 – 79.7 | 0.94 | 0.78 – 1.09 | 45.0 | 39.5 – 50.5 |
| | 4.0 | 65.1 | 56.0 – 74.2 | 1.17 | 1.07 – 1.28 | 60.0 | 52.2 – 67.8 |
| | 5.5 | 63.5 | 52.9 – 74.1 | 1.39 | 1.23 – 1.56 | 70.5 | 56.2 – 84.8 |
| PD | 2.5 | 63.7 | 57.6 – 69.8 | 0.68 | 0.51 – 0.84 | 63.0 | 57.5 – 68.5 |
| | 4.0 | 65.8 | 60.1 – 71.5 | 0.88 | 0.71 – 1.06 | 78.0 | 64.5 – 91.5 |
| | 5.5 | 54.1 | 43.5 – 64.7 | 1.01 | 0.81 – 1.22 | 93.0 | 67.7 – 118 |

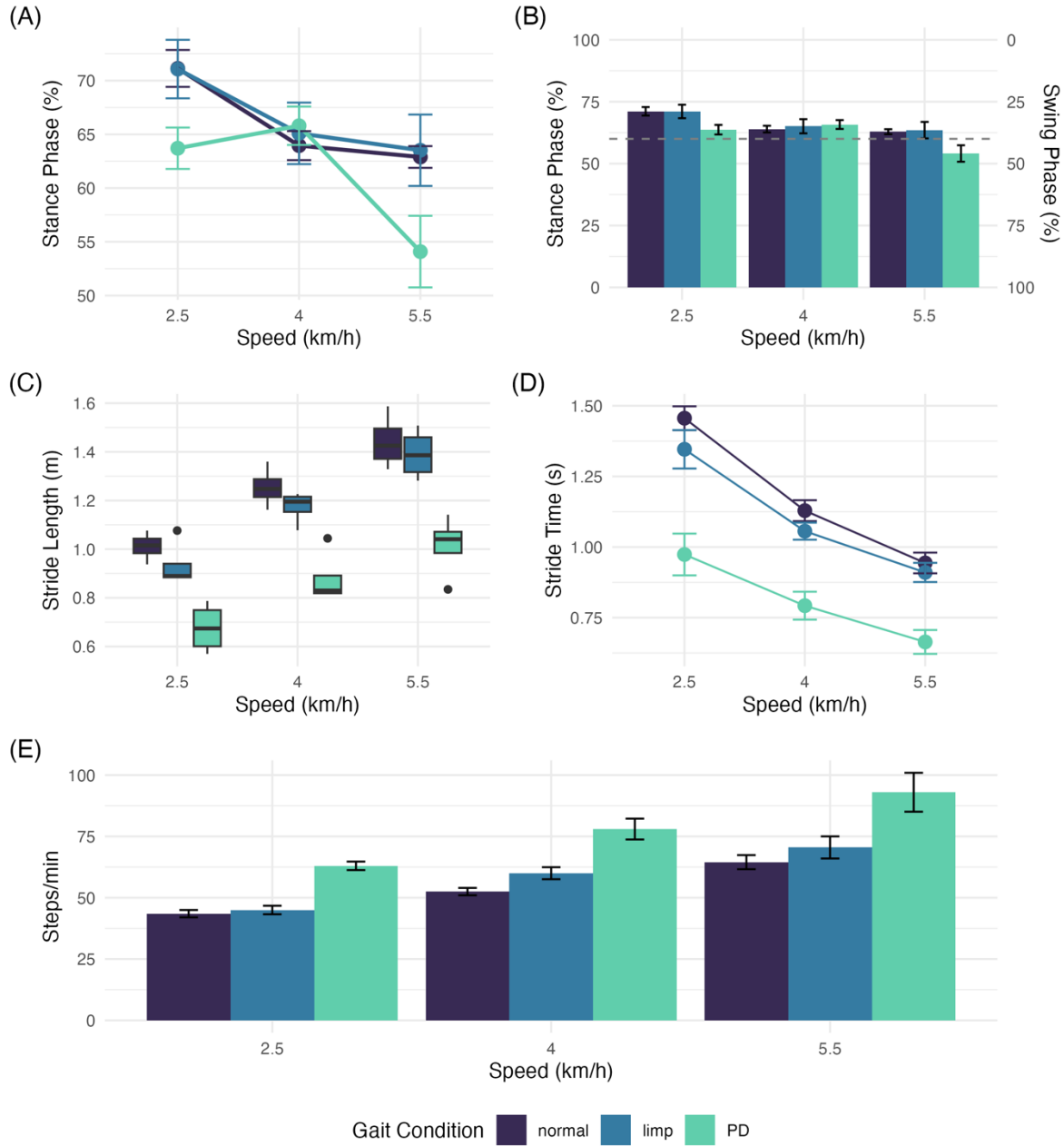


Figure 3. Spatiotemporal parameters across gait conditions. (A) Stance phase line graph. Stance phase was calculated as the proportion of frames between heel strikes (HS) and (TO). HS were detected when the ankle marker vertical position exceeded mean height by a speed-specific threshold, maintained stable vertical position across multiple frames, and vertical velocity was below a speed-specific threshold. TO were detected using the foot marker's vertical velocity exceeding predefined thresholds. These thresholds were individually optimised for each subject to ensure accurate event detection; (B) Stance-Swing ratio, calculated from stance phase percentage. Dotted line functions as a comparator, representing percentage of average stance phase (60%) when walking at 4 km/h (Hulleck et al., 2022); (C) Stride length, derived from the product of treadmill speed (converted from km/h to m/s) and calculated stride time; (D) Stride time, calculated as the interval between consecutive HS, with speed-specific minimum and maximum durations enforced to ensure valid stride detection; (E) Cadence, derived from stride frequency and expressed as steps per minute. Error bars: \pm SEM.

Figure 3A – B). All gait types showed similar relative decreases (~32%) in stance phase duration across speeds. However, unlike the steady decline observed in normal and limping gaits, PD gait showed an atypical fluctuation, with stance phase initially increasing

unexpectedly at 4 km/h before decreasing sharply at 5.5 km/h. This suggests a momentary shift in weight-bearing strategy before a more pronounced stance phase reduction at higher speeds.

Stride parameters demonstrated highly significant effects of both condition ($F(2,6) = 32.03$, $p < 0.001$) and speed ($F(2,6) = 104.04$, $p < 0.001$). Across all speeds, PD gait consistently exhibited the shortest stride length, while normal gait maintained the longest, with limping gait falling in between but closer to normal gait at all speeds. Stride length increased with speed in all conditions, but PD gait showed a notably restricted range, increasing only from 0.68 m at the slowest speed, to 1.04 m at the highest speed. By contrast, normal gait demonstrated a more pronounced stride length, increasing from 1.01 m to 1.44 m, with differences becoming most pronounced at higher speeds (31% higher than PD at 4 km/h, $p = 0.003$) (Figure 3C).

Stride time followed a similar pattern, with PD gait showing the shortest times and normal gait the longest. Normal and limping gaits showed a steeper reduction in stride time between slow and normal walking speeds, followed by a more gradual decrease between normal and fast speeds. In contrast, PD gait exhibited a more uniform decline in stride time, decreasing progressively from 0.97 s at 2.5 km/h to 0.65 s at 5.5 km/h. Despite these variations in stride characteristics, each gait pattern showed the expected compensatory relationship between stride length and time, indicating that basic mechanics were preserved across conditions (Figure 3D).

The most striking adaptation was observed in stepping frequency. Across all speeds, PD gait exhibited significantly higher cadence than both normal and limping gaits ($p = 0.001$). At 5.5 km/h, PD gait reached 92.6 steps/min, compared to normal gait at 65.4 steps/min, with limping gait falling in between but remaining much closer to normal gait (Figure 3E). Notably, while cadence differences were significant at lower speeds ($p = 0.003$ at 2.5 km/h), they became marginally non-significant at 5.5 km/h ($p = 0.055$), reflecting greater variability in PD cadence at higher speeds.

Spatiotemporal variability presented distinct patterns across gait conditions (Appendix Table 2). Normal gait demonstrated low variability in stride length, timing and cadence (CV: 5-8%), indicating a well-regulated movement pattern and predictable stepping frequency. PD gait showed the highest variability in stride length/time (CV: 12-15%) and was particularly variable for cadence (CV: 5-17%). This highlights the distinct instability patterns of PD gait,

struggling to maintain stride consistency at all speeds compared to the considerably more stable patterns of normal gait.

These results suggest that each gait condition employed distinct compensatory strategies to maintain gait speed due to underlying biomechanical differences. With PD gait, the subjects took more frequent steps to compensate for shorter strides, while in normal and limping gaits, they primarily adjusted their stride length. Despite using these different strategies, all conditions achieved similar walking speeds, demonstrating how the body adapts gait patterns to changing conditions.

3.4 Classification Analysis

LDA successfully distinguished between gait patterns with 94.4% accuracy [81.3-99.3%] in cross-validation (Appendix Figure 11). The first discriminant function accounted for 84.7% of the separation between conditions, with cadence (coefficient: 1.602) and mean stride length (-1.347) emerging as the strongest discriminative features. The classifier achieved high sensitivity across conditions (normal: 91.7%, limping: 100%, PD: 91.7%), with only two misclassifications across all trials: one normal gait and one PD gait trial were classified as limping. Mean knee angle and mean stance also contributed substantially to the classification (coefficients: 0.742 and -0.668 respectively). The robust classification performance and clear separation between conditions, particularly at lower speeds, demonstrates a reliable ability to distinguish between normal and pathological gait patterns using spatiotemporal and kinematic parameters.

4. DISCUSSION

4.1 Main Findings

This study demonstrated the capability of the smartphone-based marker system to detect and quantify differences between normal and simulated pathological gait patterns. The system successfully identified distinctive kinematic signatures, with normal gait exhibiting consistently greater knee ROM (57.5-64.5°) than both pathological conditions. Notably, the system captured speed-dependent changes in joint motion, including the reduced baseline ROM in PD gait (36.6° at 2.5 km/h) and its limited capacity to increase with speed, maintaining significantly lower values than normal gait at all speeds ($p < 0.05$).

The consistently lower knee ROM in PD gait suggests an inability to generate the necessary joint excursion for efficient walking, consistent with the rigidity and hypokinesia characteristic of Parkinsonian movement disorders (Mirelman et al., 2019). The reduced knee ROM observed in limping gait appears to be a protective mechanism to reduce weight-bearing on the affected limb (Auerbach & Tadi, 2023). This adaptation is commonly seen in clinical settings, where patients with one-sided musculoskeletal conditions modify their walking pattern to avoid pain.

The marker system proved particularly effective in quantifying spatiotemporal parameters, capturing both primary deficits and compensatory mechanisms in pathological gaits. In PD gait, the system detected both the characteristic reduction in stride length (31% reduction at 4 km/h, $p = 0.003$) and the compensatory increase in cadence (up to 92.6 steps/min vs 65.4 steps/min in normal gait). This dual detection capability is critical for understanding gait adaptation, as individuals with PD rely more on cadence modulation to maintain walking speed when stride length is impaired (Morris et al., 1998). The ability of the system to capture these distinct adjustments suggests a strong potential for clinical gait assessment, particularly in monitoring disease progression or treatment efficacy in gait disorders (Trojaniello et al., 2014).

Between-subject variability analysis revealed strong measurement consistency for normal gait, with knee ROM variability (CV: 5-8%) falling within expected range for gait studies. In contrast, higher variability observed in pathological conditions likely reflects individual differences in gait simulation rather than measurement error, as such gait variability is a consistent feature across pathological conditions (Akimoto et al., 2022; Blyton et al., 2023; Ngai & Wimmer, 2015). The system successfully tracked markers and detected gait differences even at faster walking speeds, demonstrating its potential for clinical use across a range of movement speeds.

The high classification accuracy (94.4%) achieved through LDA and maintained across cross-validation provides strong validation that this system can differentiate between normal and simulated pathological gait. The emergence of cadence and stride length as primary discriminative features aligns with clinical understanding of gait disorders, where spatiotemporal parameters often show the earliest and most consistent changes. The misclassifications occurred primarily with limping gait at higher walking speeds, suggesting that pathological gait patterns may become more difficult to distinguish as speed increases. This corresponds with the literature, where 2D systems are less effective for more complex gait analysis tasks (Michelini et al., 2020).

4.2 System Performance

The marker detection system demonstrated robust performance across all experimental conditions, successfully tracking markers in 100% of frames. Reliability was confirmed by the low CV in normal gait measurements (knee ROM CV: 5-8%; stride length CV: 5.79-7.78%), indicating consistent marker tracking with minimal measurement noise.

Measurement consistency varied with speed, with wider confidence intervals observed at higher walking speeds, particularly in pathological gaits. At 5.5 km/h, PD gait showed greater variability in cadence (CI: 67.7-118.0 steps/min) than normal gait (CI: 55.4-73.6 steps/min). Despite this, spatial measurements remained consistent, with stride length showing stable detection across speeds in normal gait (CV: 5.79-7.78%).

As expected, pathological gait conditions exhibited greater variability, particularly in ankle ROM (CV: 17-31%). This aligns with findings from Akimoto et al. (2022), suggesting that such variability reflects inherent biological differences. Despite this, the system successfully tracked markers across asymmetrical (limping) and rapid-stepping (PD) gaits, demonstrating its robustness under diverse movement patterns. However, the wider confidence intervals observed in these conditions suggest that clinical assessments should incorporate more gait cycles to enhance reliability, particularly for individuals with gait impairments.

Temporal parameters exhibited greater variability at higher speeds, particularly in pathological gait conditions, underlining their susceptibility to speed effects. This trend is consistent with findings that report higher reliability in spatial versus temporal measurements in video-based gait analysis (van Bloemendaal et al., 2019). The 60 fps sampling rate effectively captured key gait events and temporal parameters across all tested speeds, in line with motion capture standards (Michelini et al., 2020). Future smartphones with higher frame rates could improve the detection of rapid movements and provide more precise stride timing measurements at faster speeds, potentially reducing the requirements for manual calibration.

4.3 Pathological Gait Characteristics

The detected characteristics of simulated PD gait closely mirrored documented features of clinical Parkinsonian gait. The hallmark reduction in stride length (31% shorter than normal gait) and compensatory increase in cadence (92.6 vs 64.5 steps/min in normal gait) align

with the classic Parkinsonian gait pattern for both metrics (Galna et al., 2015). This shift in stepping frequency helps maintain walking speed despite restricted stride length, a well-established adaptive strategy in PD patients (Morris et al., 1996). Furthermore, the limited stride length modulation observed across speeds (ranging only from 0.68 m at 2.5 km/h to 1.04 m at 5.5 km/h) reinforces the characteristic loss of gait adaptability in PD, where individuals struggle to dynamically adjust their gait to increasing speeds (Morris et al., 1996). This restricted spatial adaptability is further compounded by reduced knee and ankle ROM, which limits joint excursion and contributes to the overall rigidity typical in PD gait (Callais Franco do Nascimento et al., 2021).

The nonlinear trend of stance phase duration across speeds in PD gait, where stance phase unexpectedly increased at 4 km/h before decreasing sharply at 5.5 km/h, may be a result of two factors. 1) Potential errors in stance phase detection: as the shuffling action of PD gait is characterised by short step height, differentiating between true TO events and subtle marker jiggle was a considerable challenge, as differences in both actions were often minor (Appendix Figures 12–15). 2) An adaptive shift in weight-bearing strategy rather than a strictly linear response to increasing speed; this pattern differs from the steady decline observed in normal and limping gaits, suggesting that individuals with PD may temporarily alter their stance phase distribution as speed increases before reaching a threshold where a sharper reduction occurs. While this could indicate biological variability, it may also arise from limitations in standardising simulated PD gait. Given the well-documented inconsistencies in Parkinsonian gait mechanics (Frenkel-Toledo et al., 2005), further research involving individuals with PD is necessary to determine whether these fluctuations are intrinsic to PD gait dynamics, a result of the simulation process, or data processing errors.

Simulated limping gait demonstrated the expected asymmetrical loading pattern, with anterior-posterior marker progression suggesting modifications in swing phase strategies. Stride length in limping gait followed a similar progression to normal gait across speeds rather than exhibiting a pronounced reduction, as seen in some clinical cases (Shushtari et al., 2022). These patterns may differ from those of genuine patients, who develop long-term compensatory strategies. The increase in movement variability with speed (CV: 7.7-12.8%) suggests that maintaining consistent asymmetrical walking became harder at faster speeds. This aligns with clinical findings that report speed-dependent gait instability in lower limb pathologies, where maintaining compensatory mechanics becomes increasingly challenging under dynamic conditions (Walha et al., 2022). The increase in variability at faster speeds

may reflect a reduced ability to maintain a stable asymmetric gait, potentially due to increased demand on neuromuscular control mechanisms.

4.4 Clinical Implications

This smartphone-based system provides an affordable and accessible option for measuring gait in clinical settings without access to traditional motion capture systems. The ability to successfully detect changes in movement patterns and timing make it potentially suitable for initial assessments and tracking patient progress during rehabilitation. The reliability across walking speeds enhances its utility for monitoring treatment outcomes.

The portability of this system allows for gait assessment in various clinical settings, from rehabilitation centres to patients' homes, unlike traditional laboratory-based equipment. While this flexibility could facilitate multi-site research and wider clinical access, it requires careful standardisation of testing conditions. Maintaining consistent camera placement, lighting, and background across different environments presents a key challenge.

The system provides a considerable cost reduction in gait analysis technology, with equipment totalling under £1000, compared to tens of thousands of pounds for traditional motion capture systems (Romero et al., 2017). Combined with minimal training requirements, this cost reduction makes quantitative gait analysis more accessible to smaller clinics and resource-limited settings.

Recent advancements have been made in markerless motion capture (MMC), where tracking accuracy has greatly improved. OpenCap, a smartphone-based video capture system, has been validated against gold-standard marker-based systems (Turner et al., 2024). Interestingly, OpenCap performs comparably with marker-based systems in the sagittal plane for several metrics, such as flexion-extension estimation (Turner et al., 2024). However, OpenCap has been shown to slightly overestimate joint angles, particularly in sagittal plane movements, and may require extensive calibration for clinical use.

Given these considerations, a smartphone-based marker system offers advantages over current MMC systems when greater control over detection accuracy is required. These minor inaccuracies may be particularly relevant when assessing individuals with pathological gait, where small deviations in joint angles can be clinically significant. While markerless systems offer a promising low-cost approach, this marker-based system provides more reliable

movement tracking without algorithmic drift or noise. Future research could explore combining approaches to achieve both greater affordability and precision.

4.5 Limitations and Future Directions

Several limitations of this study should be acknowledged. The small sample size ($n = 4$) and young age range (22-26 years) restrict generalisability to broader populations, particularly older individuals who are typically affected by neurological and musculoskeletal gait impairments. However, the large effect sizes and consistency of observed patterns suggest meaningful differences were detectable despite the limited sample.

A key technical limitation was the challenge of detecting stance phases in PD gait, where the characteristic shuffling motion and reduced stride length complicated marker tracking. While speed-specific thresholds were implemented to improve detection accuracy, the foot's lower clearance and prolonged ground contact contributed to occasional misclassification of stance and swing phases. Future implementations might benefit from using flat reflective markers instead of spherical markers to enhance contrast and reduce detection errors caused by shadows and jiggling motion.

As a proof-of-concept study, relying on simulated rather than true pathological gait patterns is an important limitation. While participants followed standard instructions, their simulations likely failed to capture the full complexity of true pathological gaits, particularly for features such as freezing of gait in PD. Additionally, the constraint of arm positioning – while necessary for marker visibility – may have altered natural movement patterns, potentially affecting measured parameters.

Several key directions for future research emerge from this study. Validation with clinical populations across a broader age range is essential, particularly in individuals with neurological and musculoskeletal gait impairments. Likewise this system must be validated against established motion capture technologies. Finally, developing automated tracking capabilities and calibration through machine learning would minimise time constraints.

5. CONCLUSION

These findings demonstrate that a low-cost 2D de novo smartphone-based marker-based system can differentiate between normal and simulated pathological gait. Key differences

included reduced joint and spatial movement range in pathological conditions. Movement variability analysis revealed strong measurement consistency for normal gait, while higher variability in pathological conditions was possibly due to individual differences in gait simulation.

As this system requires common equipment at a fraction of the cost of traditional motion capture systems, it provides an accessible approach to clinical gait assessment. The combination of portability and straightforward implementation makes quantitative gait analysis feasible for smaller clinics and settings with limited resources. Although further validation with a larger sample size and more representative populations is needed due to the use of simulated gaits in this study, this system shows promise in bridging the gap between simple observational methods and expensive laboratory equipment, potentially making objective gait analysis available to a broader range of clinical settings.

REFERENCES

Akimoto, T., Kawamura, K., Wada, T., Ishihara, N., Yokota, A., Suginoshita, T., & Yokoyama, S. (2022). Gait cycle time variability in patients with knee osteoarthritis and its possible associating factors. *Journal of Physical Therapy Science*, 34(2), 140–145.
<https://doi.org/10.1589/jpts.34.140>

Andrysek, J., Redekop, S., & Naumann, S. (2007). Preliminary evaluation of an automatically stance-phase controlled pediatric prosthetic knee joint using quantitative gait analysis. *Archives of Physical Medicine and Rehabilitation*, 88(4), 464–470.
<https://doi.org/10.1016/j.apmr.2007.01.009>

Auerbach, N., & Tadi, P. (2023). *Antalgic gait in adults*. In *StatPearls*. StatPearls Publishing. Retrieved [January 31, 2025], from: <https://www.ncbi.nlm.nih.gov/books/NBK559243/>

Belda-Lois, J.-M., Mena-del Horno, S., Bermejo-Bosch, I., Moreno, J. C., Pons, J. L., Farina, D., Iosa, M., Molinari, M., Tamburella, F., Ramos, A., Caria, A., Solis-Escalante, T., Brunner, C., & Rea, M. (2011). Rehabilitation of gait after stroke: a review towards a top-down approach. *Journal of NeuroEngineering and Rehabilitation*, 8(1), 66.
<https://doi.org/10.1186/1743-0003-8-66>

Ben-Shachar, M. S., Lüdecke, D., Makowski, D. (2020). Effectsize: estimation of effect sizes and indices. *Journal of Open Source Software*, 5(56), 2815.

<http://doi.org/10.21105/joss.02815>

Benedetti, M. G., Beghi, E., De Tanti, A., Cappozzo, A., Basaglia, N., Cutti, A. G., Cereatti, A., Stagni, R., Verdini, F., Manca, M., Fantozzi, S., Mazzà, C., Camomilla, V., Campanini, I., Castagna, A., Cavazzuti, L., Del Maestro, M., Croce, U. D., Gasperi, M., Leo, T., ... Ferrarin, M. (2017). SIAMOC position paper on gait analysis in clinical practice: General requirements, methods and appropriateness. Results of an Italian consensus conference.

Gait & Posture, 58, 252–260. <https://doi.org/10.1016/j.gaitpost.2017.08.003>

van Bloemendaal, M., Beelen, A., Kleissen, R. F. M., Geurts, A. C., Nollet, F., & Bus, S. A. (2019). Concurrent validity and reliability of a low-cost gait analysis system for assessment of spatiotemporal gait parameters. *Journal of Rehabilitation Medicine*, 51(6), 456–463.

<https://doi.org/10.2340/16501977-2559>

Blyton, S. J., Snodgrass, S. J., Pizzari, T., Birse, S. M., Likens, A. D., & Edwards, S. (2023). The impact of previous musculoskeletal injury on running gait variability: A systematic review. *Gait & Posture*, 101, 124–133. <https://doi.org/10.1016/j.gaitpost.2023.01.018>

Callais Franco do Nascimento, T., Martins Gervásio, F., Pignolo, A., Augusto Santos Bueno, G., Araújo do Carmo, A., Martins Ribeiro, D., D'Amelio, M., & Augusto Dos Santos Mendes, F. (2021). Assessment of the kinematic adaptations in Parkinson's disease using the gait profile score: influences of trunk posture, a pilot study. *Brain Sciences*, 11(12), 1605.

<https://doi.org/10.3390/brainsci11121605>

Cappozzo, A. (1984). Gait analysis methodology. *Human Movement Science*, 3(1-2), 27-50. [https://doi.org/10.1016/0167-9457\(84\)90004-6](https://doi.org/10.1016/0167-9457(84)90004-6)

Fatone, S., & Stine, R. (2015). Capturing quality clinical videos for two-dimensional motion analysis. *Journal of Prosthetics and Orthotics*, 27(1), 27-32.

<https://doi.org/10.1097/JPO.0000000000000051>

Frenkel-Toledo, S., Giladi, N., Peretz, C., Herman, T., Gruendlinger, L., & Hausdorff, J. M. (2005). Effect of gait speed on gait rhythmicity in Parkinson's disease: variability of stride time and swing time respond differently. *Journal of Neuroengineering and Rehabilitation*, 2, 23. <https://doi.org/10.1186/1743-0003-2-23>

Galna, B., Lord, S., Burn, D. J., & Rochester, L. (2015). Progression of gait dysfunction in incident Parkinson's disease: impact of medication and phenotype. *Movement Disorders : Official Journal of the Movement Disorder Society*, 30(3), 359–367.

<https://doi.org/10.1002/mds.26110>

García-Pinillos, F., Soto-Hermoso, V. M., & Latorre-Román, P. Á. (2016). Do running kinematic characteristics change over a typical HIIT for endurance runners?. *Journal of Strength and Conditioning Research*, 30(10), 2907–2917.

<https://doi.org/10.1519/JSC.0000000000001380>

Gehlsen, G., Beekman, K., Assmann, N., Winant, D., Seidle, & M., Carter A. (1986). Gait characteristics in multiple sclerosis: progressive changes and effects of exercise on parameters. *Archives of Physical Medicine and Rehabilitation*, 67, 536–539.

Hobart, J.C., Riazi, A., Lamping, D.L., Fitzpatrick, R., & Thompson, A.J. (2003). Measuring the impact of MS on walking ability: the 12-item MS walking scale (MSWS-12). *Neurology*, 60, 31–36. <http://doi.org/10.1212/WNL.60.1.31>

Horsak, B., Eichmann, A., Lauer, K., Prock, K., Krondorfer, P., Siragy, T., & Dumphart, B. (2023). Concurrent validity of smartphone-based markerless motion capturing to quantify lower-limb joint kinematics in healthy and pathological gait. *Journal of Biomechanics*, 159, 111801. <https://doi.org/10.1016/j.jbiomech.2023.111801>

Hulleck, A.A., Mohan, D. M., Abdallah, N., El Rich, M., & Khalaf, K. (2022). Present and future of gait assessment in clinical practice: towards the application of novel trends and technologies. *Frontiers in Medical Technology*, 4. <http://doi.org/10.3389/fmedt.2022.901331>

Intzandt, B., Beck, E. N., & Silveira, C. R. A. (2018). The effects of exercise on cognition and gait in Parkinson's Disease: a scoping review. *Neuroscience and Biobehavioral Reviews*, 95, 136–69. <https://doi.org/10.1016/j.neubiorev.2018.09.018>

Kassambara, A. (2024). *rstatix: Pipe-friendly framework for basic statistical tests*. (Version 0.7.2) [R package]. Comprehensive R Archive Network (CRAN). <https://CRAN.R-project.org/package=rstatix>

Lawrence M.A. (2016). *ez: Easy analysis and visualization of factorial experiments*. (Version 4.4-0) [R package]. Comprehensive R Archive Network (CRAN). <https://CRAN.R-project.org/package=ez>

Mathias, S., Nayak, U. S., & Isaacs, B. (1986). Balance in elderly patients: the "get-up and go" test. *Archives of Physical Medicine and Rehabilitation*, 67(6), 387–389.

Michelini, A., Eshraghi, A., & Andrysek, J. (2020). Two-dimensional video gait analysis. *Prosthetics and Orthotics International*, 44(4), 245–262.

<http://doi.org/10.1177/0309364620921290>

Min, Y. S., Jung, T. D., Lee, Y. S., Kwon, Y., Kim, H. J., Kim, H. C., Lee, J. C., & Park, E. (2024). Biomechanical gait analysis using a smartphone-based motion capture system (OpenCap) in patients with neurological disorders. *Bioengineering (Basel, Switzerland)*, 11(9), 911. <https://doi.org/10.3390/bioengineering11090911>

Mirelman, A., Bonato, P., Camicioli, R., Ellis, T. D., Giladi, N., Hamilton, J. L., Hass, C. J., Hausdorff, J. M., Pelosin, E., & Almeida, Q. J. (2019). Gait impairments in Parkinson's disease. *The Lancet. Neurology*, 18(7), 697–708. [https://doi.org/10.1016/S1474-4422\(19\)30044-4](https://doi.org/10.1016/S1474-4422(19)30044-4)

Morris, M. E., Iansek, R., Matyas, T. A., & Summers, J. J. (1996). Stride length regulation in Parkinson's disease. Normalization strategies and underlying mechanisms. *Brain: A Journal of Neurology*, 119 (Pt 2), 551–568. <https://doi.org/10.1093/brain/119.2.551>

Morris, M., Iansek, R., Matyas, T., & Summers, J. (1998). Abnormalities in the stride length-cadence relation in Parkinsonian gait. *Movement Disorders : Official Journal of the Movement Disorder Society*, 13(1), 61–69. <https://doi.org/10.1002/mds.870130115>

Ngai, V., & Wimmer, M. A. (2015). Variability of TKR knee kinematics and relationship with gait kinetics: implications for total knee wear. *BioMed Research International*, 2015, 284513. <https://doi.org/10.1155/2015/284513>

Ooms, J. (2023). *av: Working with audio and video in R* (Version 0.9.0) [R package]. Comprehensive R Archive Network (CRAN). <https://CRAN.R-project.org/package=av>

Romero, V., Amaral, J., Fitzpatrick, P., Schmidt, R. C., Duncan, A. W., & Richardson, M. J. (2017). Can low-cost motion-tracking systems substitute a Polhemus system when researching social motor coordination in children?. *Behavior Research Methods*, 49(2), 588–601. <https://doi.org/10.3758/s13428-016-0733-1>

Scataglini, S., Abts, E., Van Bocxlaer, C., Van den Bussche, M., Meletani, S., & Truijen, S. (2024). Accuracy, validity, and reliability of markerless camera-based 3D motion capture systems versus marker-based 3D motion capture systems in gait analysis: a systematic review and meta-analysis. *Sensors (Basel, Switzerland)*, 24(11), 3686.

<https://doi.org/10.3390/s24113686>

Sethi, D., Bharti, S., & Prakash, C. (2022). A comprehensive survey on gait analysis: history, parameters, approaches, pose estimation, and future work. *Artificial Intelligence in Medicine*, 129, 102314. <https://doi.org/10.1016/j.artmed.2022.102314>

Shushtari, M., Dinovitzer, H., Weng, J., & Arami, A. (2022). Ultra-robust real-time estimation of gait phase. *IEEE Transactions on Neural Systems and Rehabilitation Engineering: a Publication of the IEEE Engineering in Medicine and Biology Society*, 30, 2793–2801. <https://doi.org/10.1109/TNSRE.2022.3207919>

Snijders, A.H., van de Warrenburg. B.P., Giladi, N., & Bloem, B. R. (2007). Neurological gait disorders in elderly people: clinical approach and classification. *Lancet Neurology*, 6(1):63–74. [http://doi.org/10.1016/S1474-4422\(06\)70678-0](http://doi.org/10.1016/S1474-4422(06)70678-0)

Stolze, H., Klebe, S., Petersen, G., Raethjen, J., Wenzelburger, R., Witt, K., & Deuschl, G. (2002). Typical features of cerebellar ataxic gait. *Journal of Neurology, Neurosurgery & Psychiatry*, 73(3), 310–312. <https://doi.org/10.1136/jnnp.73.3.310>

Tinetti, M.E. (1986). Performance-oriented assessment of mobility problems in elderly patients. *Journal of the American Geriatrics Society*, 34, 119–126.

<http://doi.org/10.1111/j.1532-5415.1986.tb05480.x>

Trojaniello, D., Cereatti, A., Pelosin, E., Avanzino, L., Mirelman, A., Hausdorff, J. M., & Della Croce, U. (2014). Estimation of step-by-step spatio-temporal parameters of normal and impaired gait using shank-mounted magneto-inertial sensors: application to elderly, hemiparetic, Parkinsonian and choreic gait. *Journal of Neuroengineering and Rehabilitation*, 11, 152. <https://doi.org/10.1186/1743-0003-11-152>

Turner, J. A., Chaaban, C. R., & Padua, D. A. (2024). Validation of OpenCap: A low-cost markerless motion capture system for lower-extremity kinematics during return-to-sport tasks. *Journal of Biomechanics*, 171, 112200.

<https://doi.org/10.1016/j.jbiomech.2024.112200>

Walha, R., Gaudreault, N., Dagenais, P., & Boissy, P. (2022). Spatiotemporal parameters and gait variability in people with psoriatic arthritis (PsA): a cross-sectional study. *Journal of Foot and Ankle Research*, 15(1), 19. <https://doi.org/10.1186/s13047-022-00521-y>

Wang, J., Xu, W., Wu, Z., Zhang, H., Wang, B., Zhou, Z., Wang, C., Li, K., & Nie, Y. (2025). Evaluation of a smartphone-based markerless system to measure lower-limb kinematics in patients with knee osteoarthritis. *Journal of Biomechanics*, 181, 112529. Advance online publication. <https://doi.org/10.1016/j.jbiomech.2025.112529>

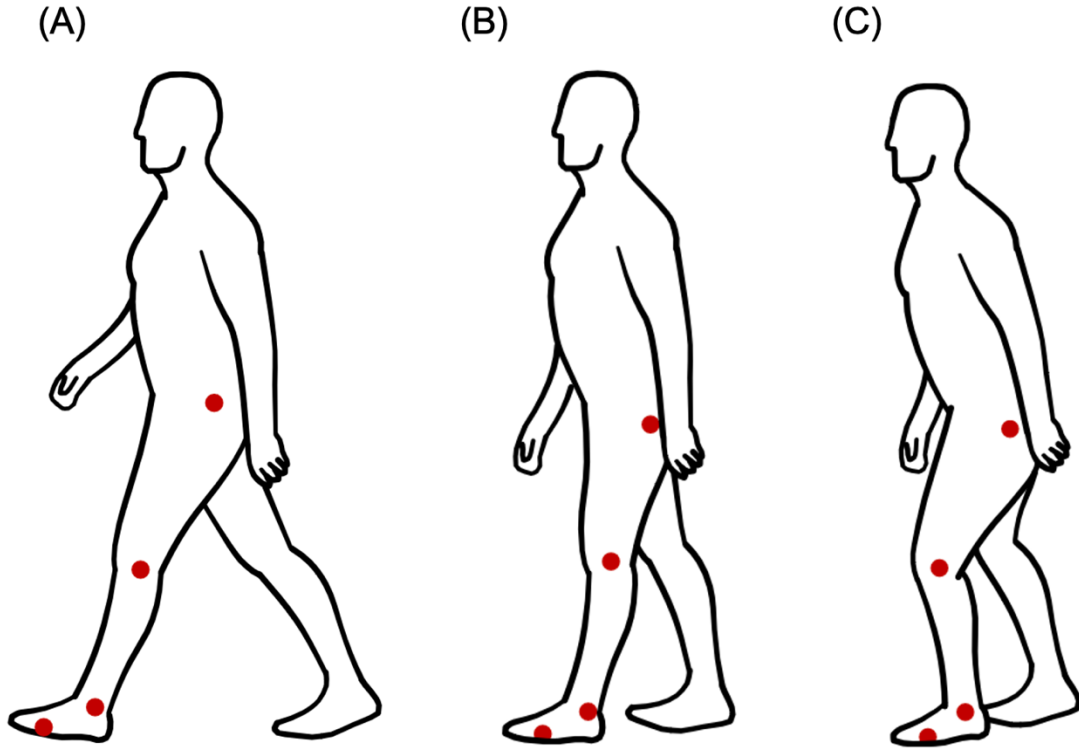
APPENDIX

Appendix Table 1. Between-Subject Kinematic Coefficient of Variation (CV)

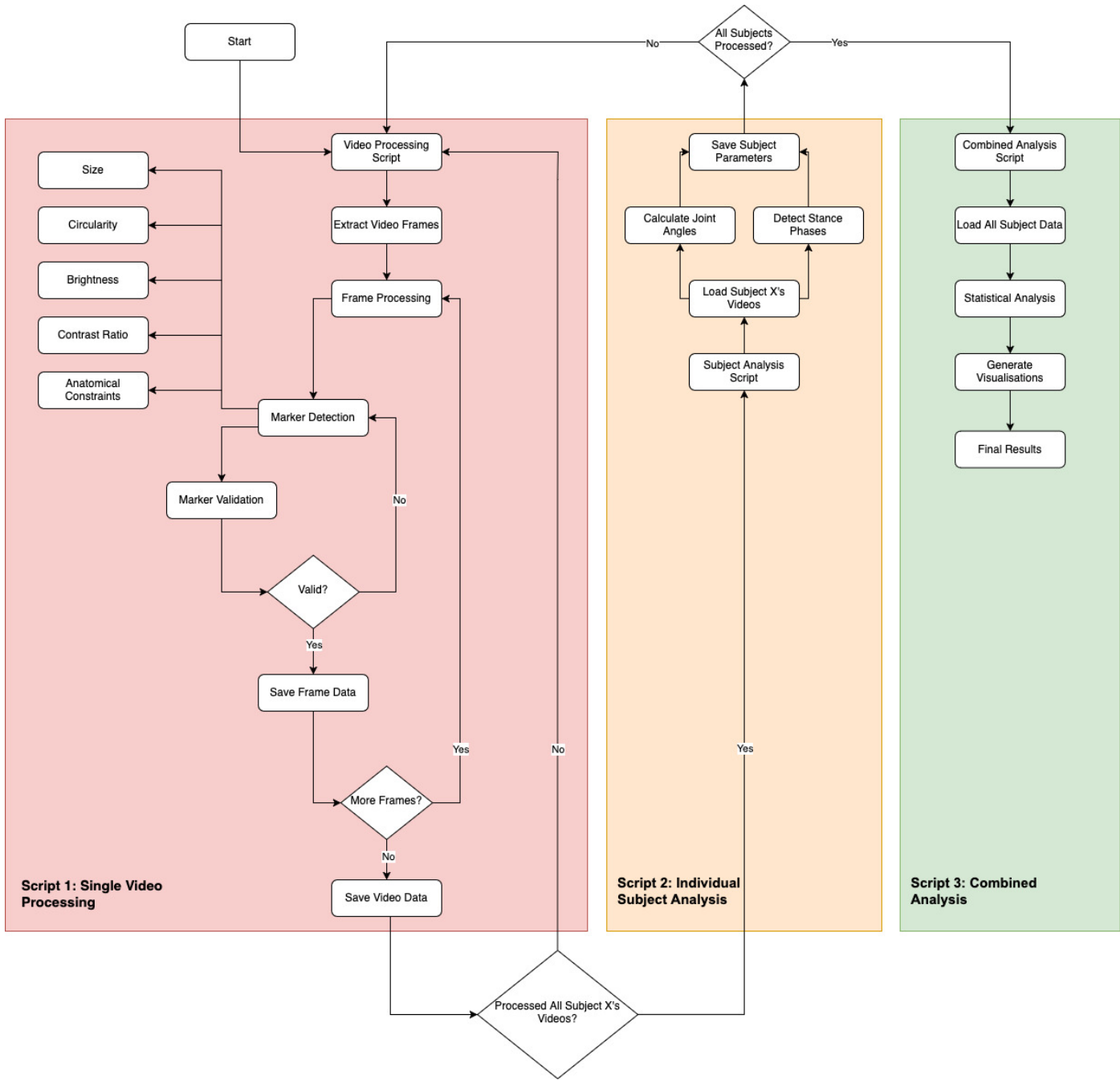
| Condition | Speed (km/h) | CV % | |
|-----------|--------------|----------|-----------|
| | | Knee ROM | Ankle ROM |
| normal | 2.5 | 8.45 | 18.1 |
| | 4.0 | 5.44 | 17.1 |
| | 5.5 | 5.05 | 22.0 |
| limp | 2.5 | 15.9 | 29.2 |
| | 4.0 | 8.60 | 31.0 |
| | 5.5 | 7.99 | 26.5 |
| PD | 2.5 | 27.3 | 29.6 |
| | 4.0 | 19.2 | 28.7 |
| | 5.5 | 14.9 | 25.4 |

Appendix Table 2. Between-Subject Spatiotemporal Coefficient of Variation (CV)

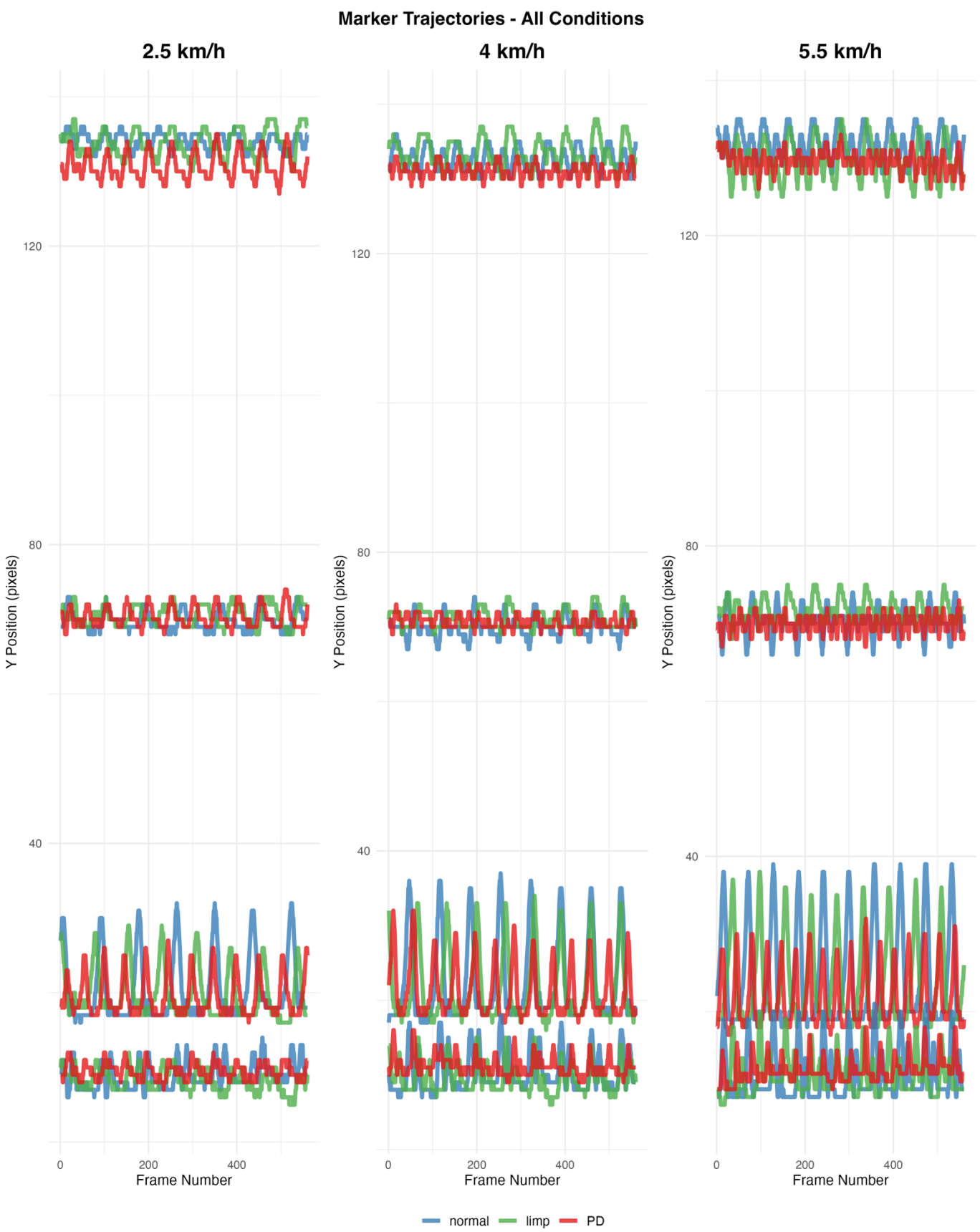
| Condition | Speed (km/h) | CV % | |
|-----------|--------------|--------------------|---------|
| | | Stride Length/Time | Cadence |
| normal | 2.5 | 5.79 | 6.90 |
| | 4.0 | 6.55 | 5.71 |
| | 5.5 | 7.78 | 8.91 |
| limp | 2.5 | 10.1 | 7.70 |
| | 4.0 | 5.71 | 8.16 |
| | 5.5 | 7.47 | 12.8 |
| PD | 2.5 | 15.2 | 5.50 |
| | 4.0 | 12.5 | 10.9 |
| | 5.5 | 12.7 | 17.1 |



Appendix Figure 1. Three Walking Gaits With Markers. Participants were instructed to walk at three different walking speeds: slow (2.5 km/h), medium (4 km/h) and fast (5.5 km/h) performing three gait conditions (normal, simulated limping, and simulated Parkinsonian gait). Participants would start with a normal walking gait at the slowest speed, then medium speed, and finally fast speed, before repeating the cycle for limping and Parkinsonian gait. Standardised rest periods of 20 seconds between speeds were implemented, with 60 seconds rest between conditions. Familiarisation with each gait was done prior to any recorded task, and familiarisation periods of 10 seconds were given at the end of each rest period and prior to recording to ensure consistency in gait patterns. A total of nine tasks were performed per subject. (A) Normal walking gait; (B) Antalgic limping gait (simulated): participants were instructed to affect a limp reducing weight-bearing on the left (measured) side to replicate pain avoidance; (C) Parkinsonian gait (simulated): participants were instructed to affect a shuffling gait by reducing their stepping height and step length, keeping knees slightly bent.

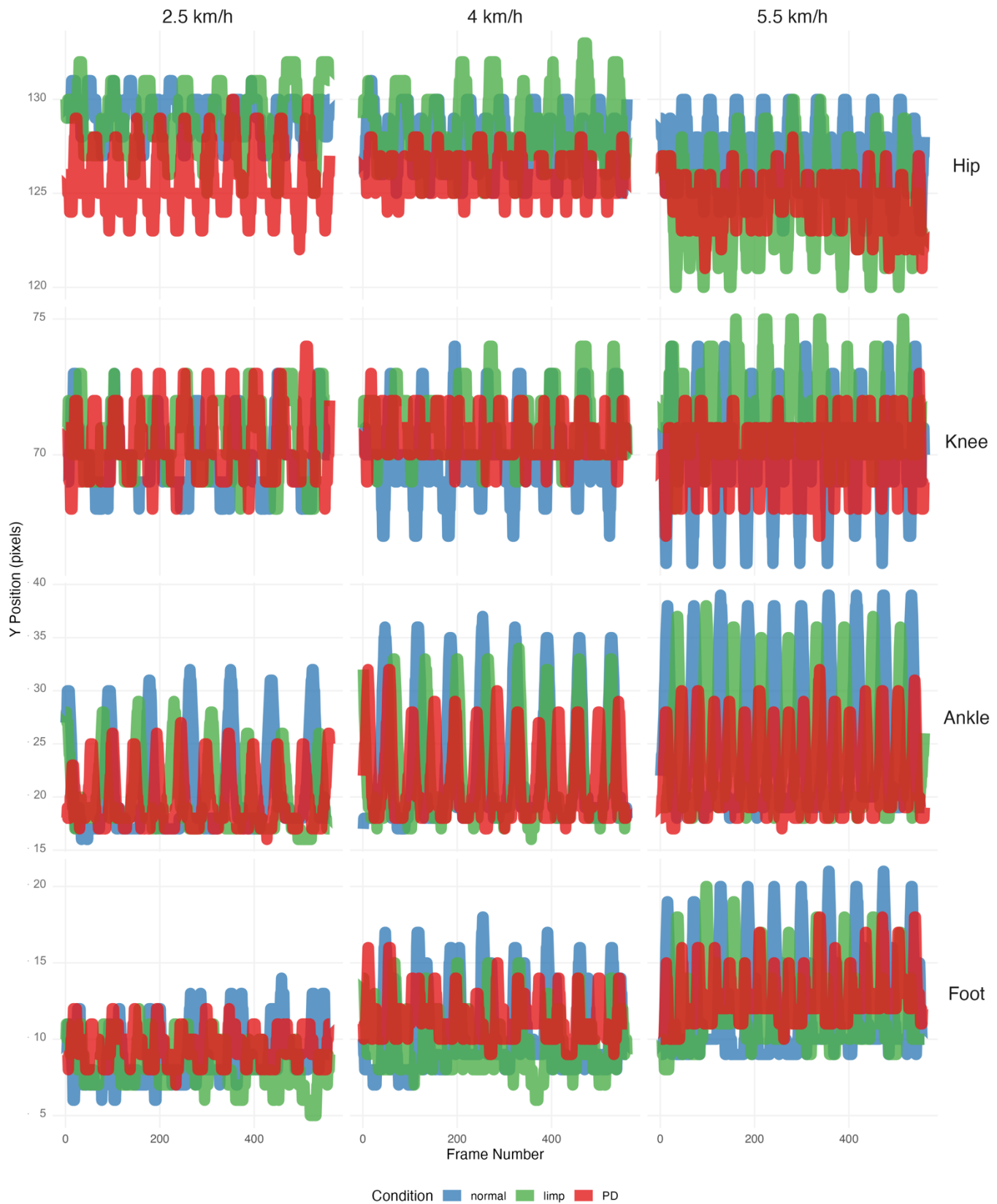


Appendix Figure 2. Software Framework Workflow Diagram With Three-Stage Analysis Pipeline. Script 1 (red): processes individual videos through frame extraction, marker detection, and validation using five criteria; Script 2 (orange): collates and analyses individual subject data by calculating joint angles and detecting stance phases across all nine videos per subject; Script 3 (green): combined analysis of all four subjects for statistical analysis and visualisation generation. Diamond shapes indicate decision points in the workflow.

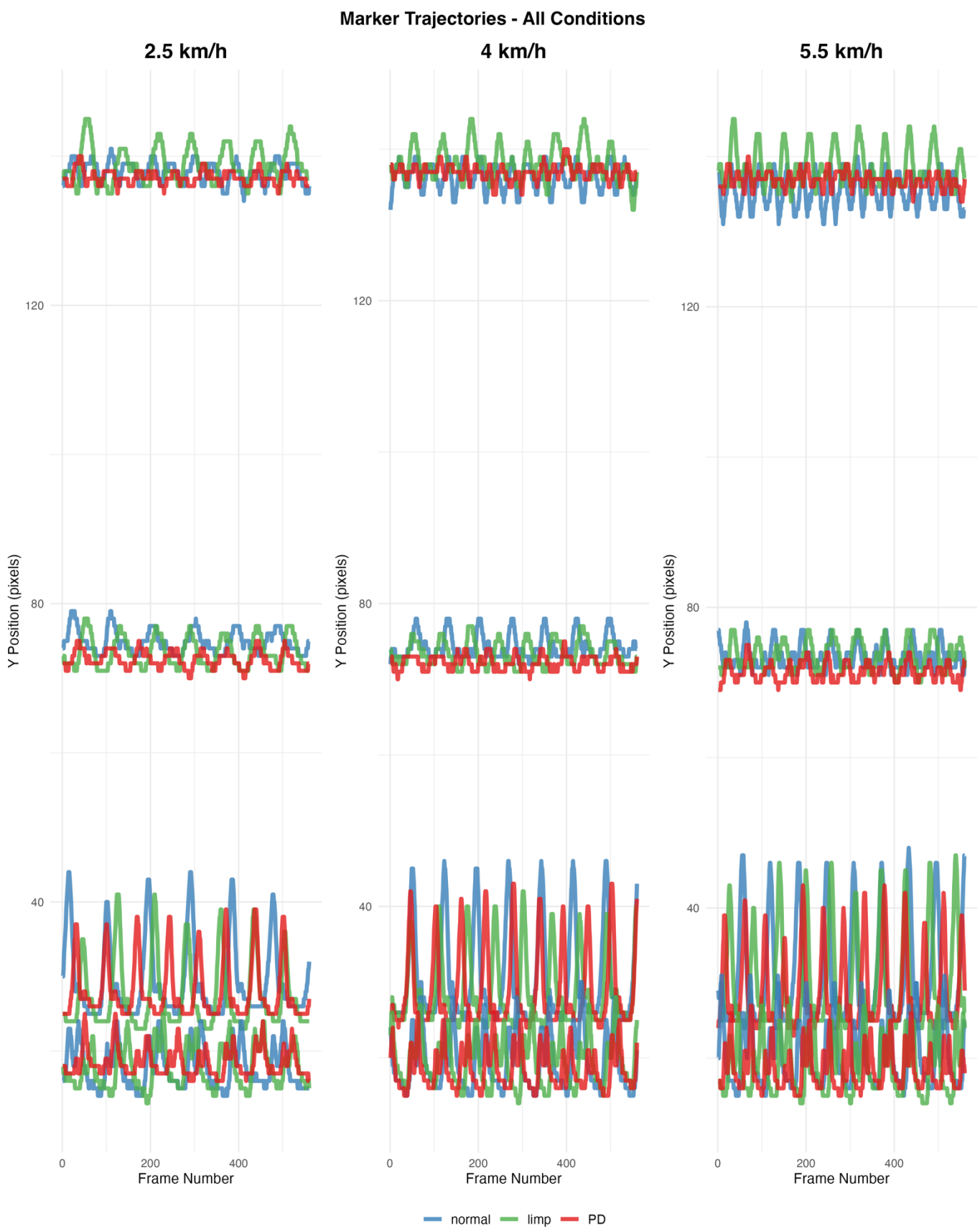


Appendix Figure 3. Marker Trajectory, Subject 1. All four markers plotted together with direct comparison of normal, limping and Parkinsonian gait across 2.5, 4, and 5.5 km/h.

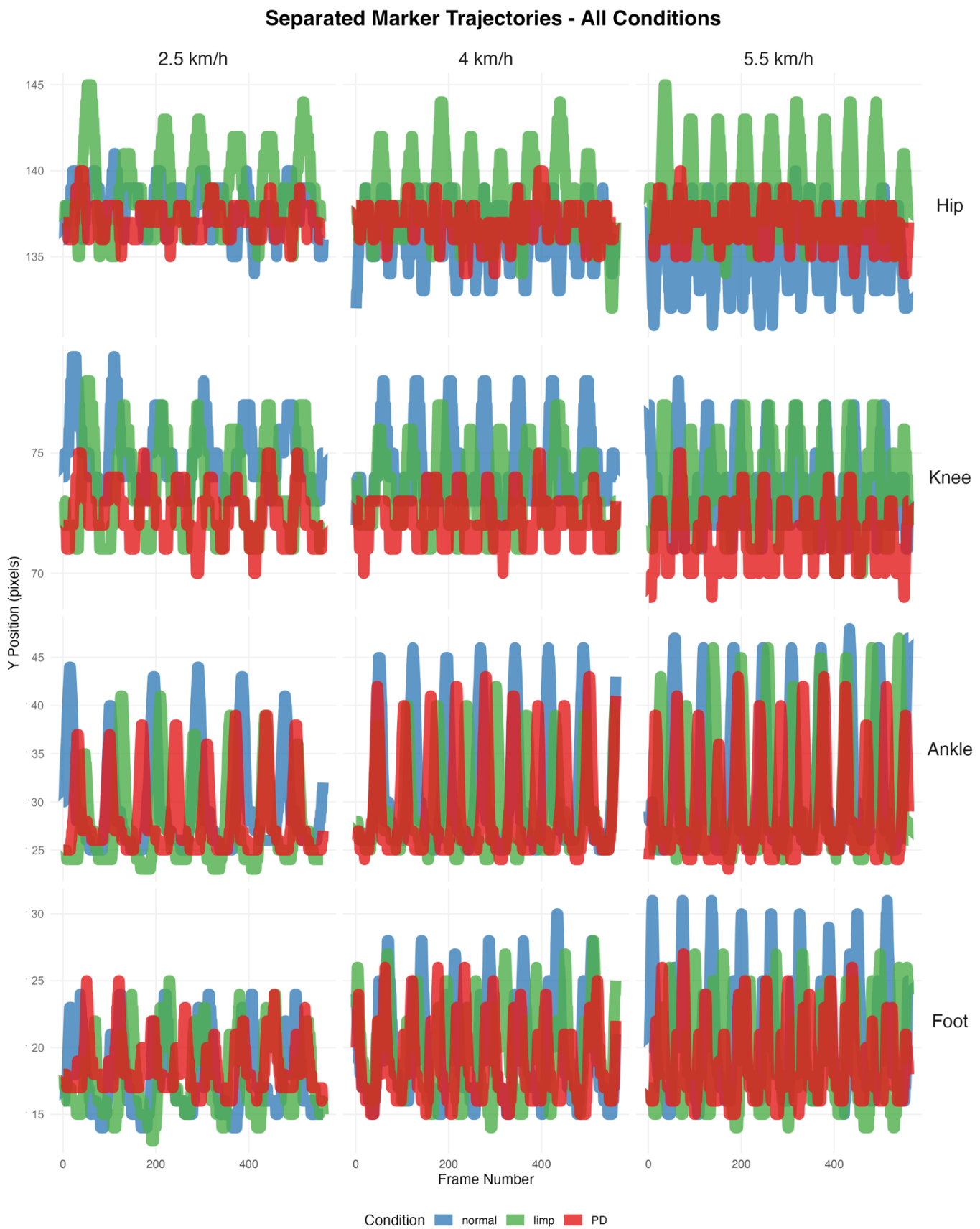
Separated Marker Trajectories - All Conditions



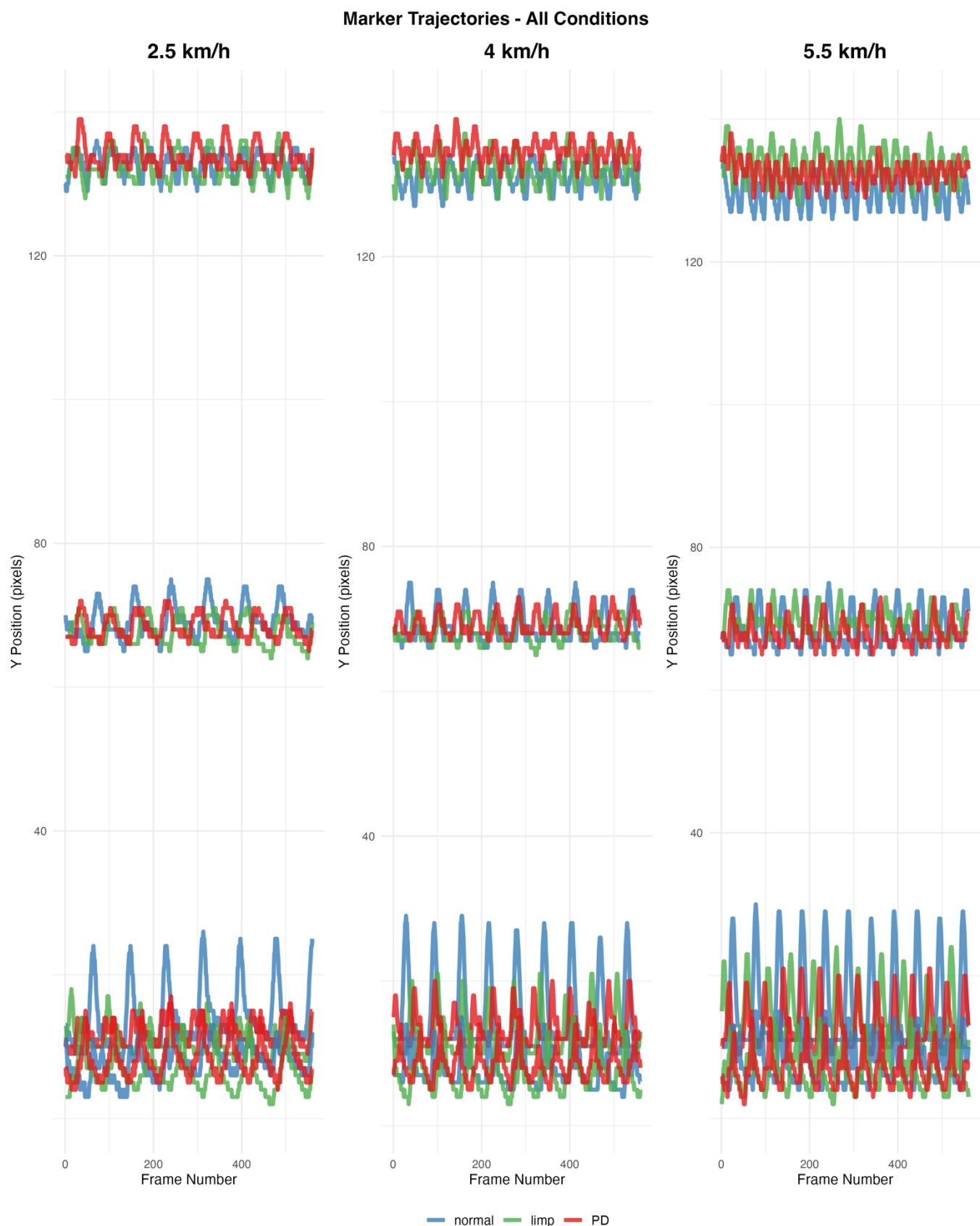
Appendix Figure 4. Marker Trajectory, Subject 1. All four markers plotted separately to enhance interpretability, with direct comparison of normal, limping and Parkinsonian gait across 2.5, 4, and 5.5 km/h. Marginal changes in baseline Y position of markers between or within speeds over time a result of slight camera tilt produced between recordings.



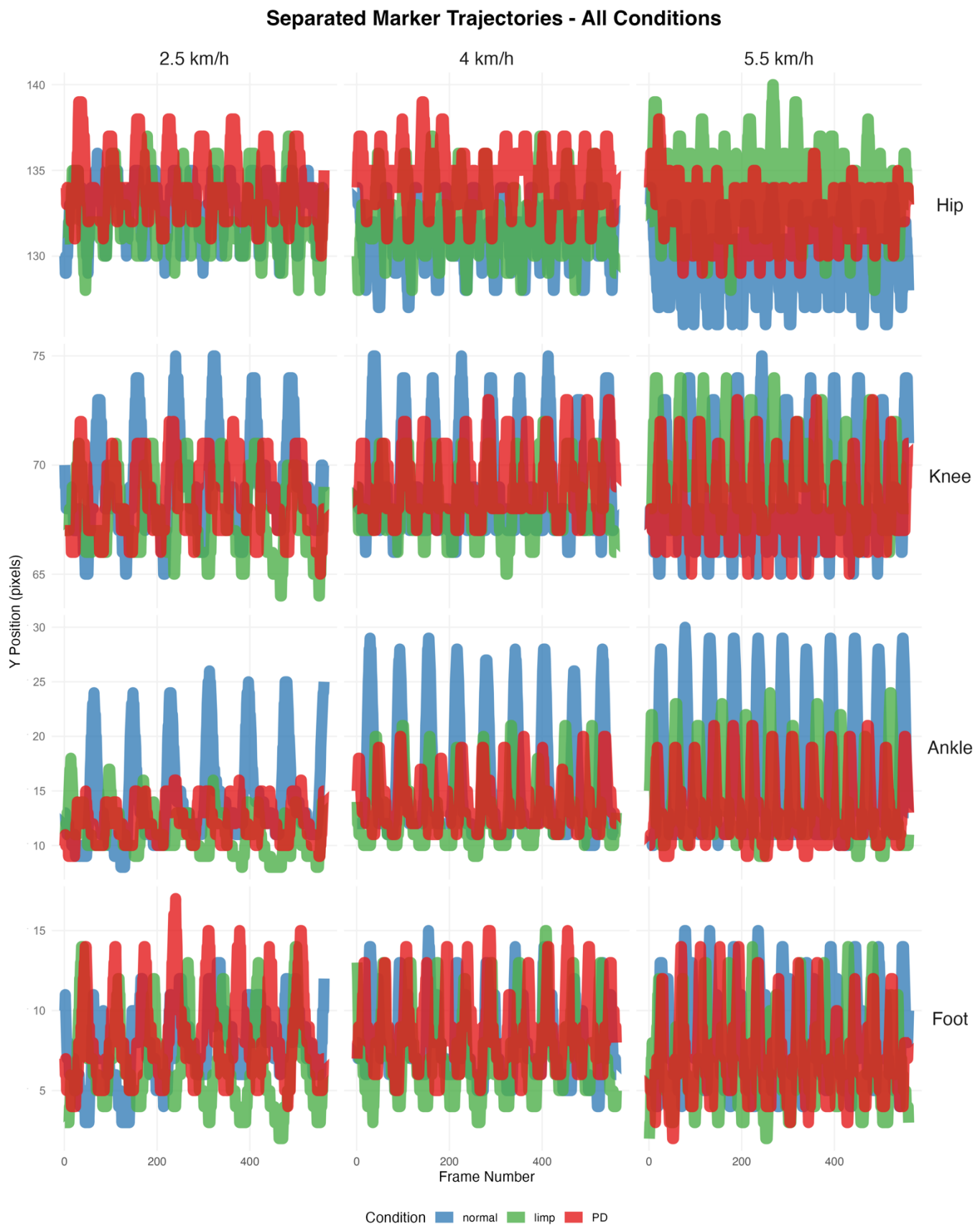
Appendix Figure 5. Marker Trajectory, Subject 2. All four markers plotted together, with direct comparison of normal, limping and Parkinsonian gait across 2.5, 4, and 5.5 km/h.



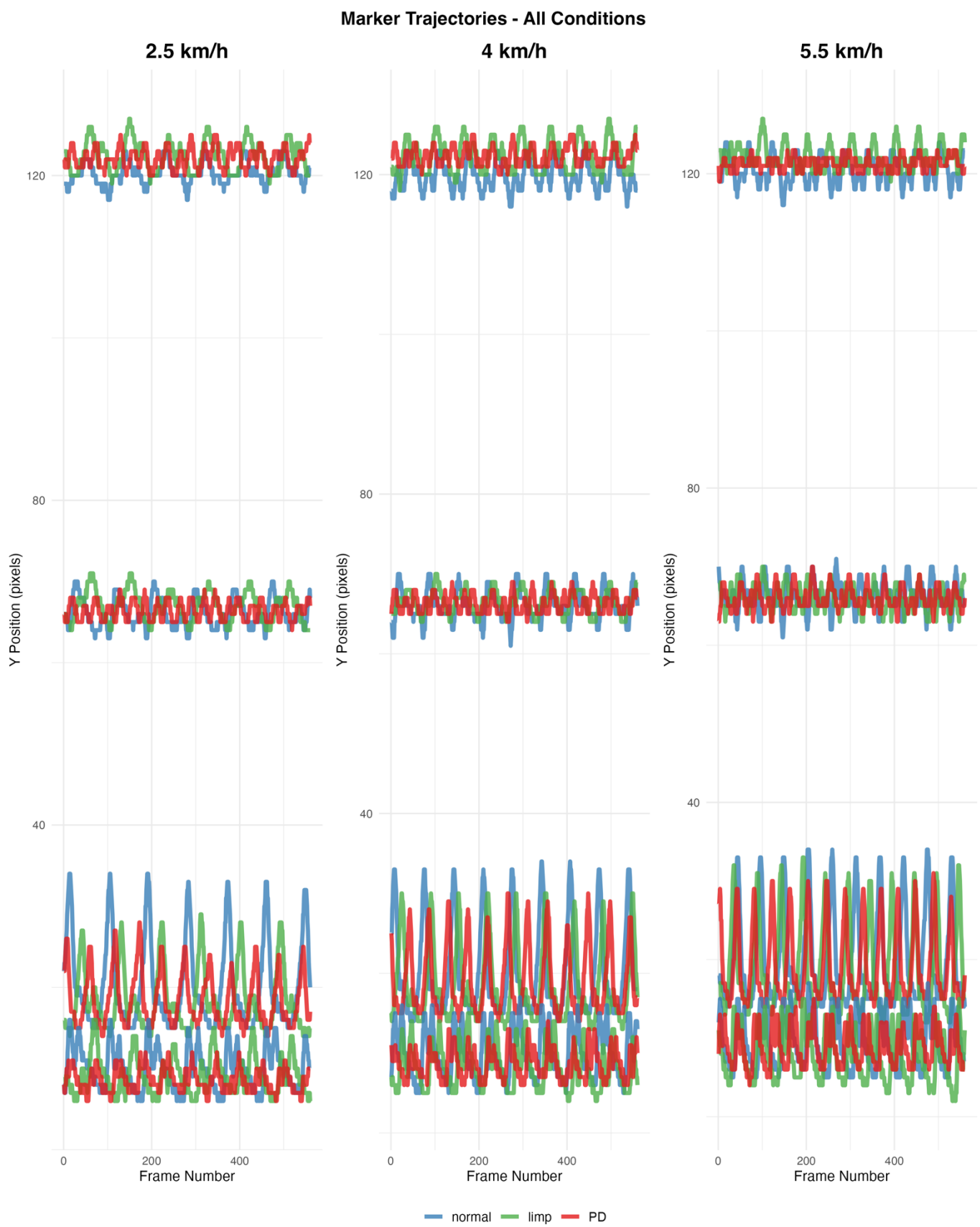
Appendix Figure 6. Marker Trajectory, Subject 2. All four markers plotted separately to enhance interpretability, with direct comparison of normal, limping and Parkinsonian gait across 2.5, 4, and 5.5 km/h. Marginal changes in baseline Y position of markers between or within speeds over time a result of slight camera tilt produced between recordings.



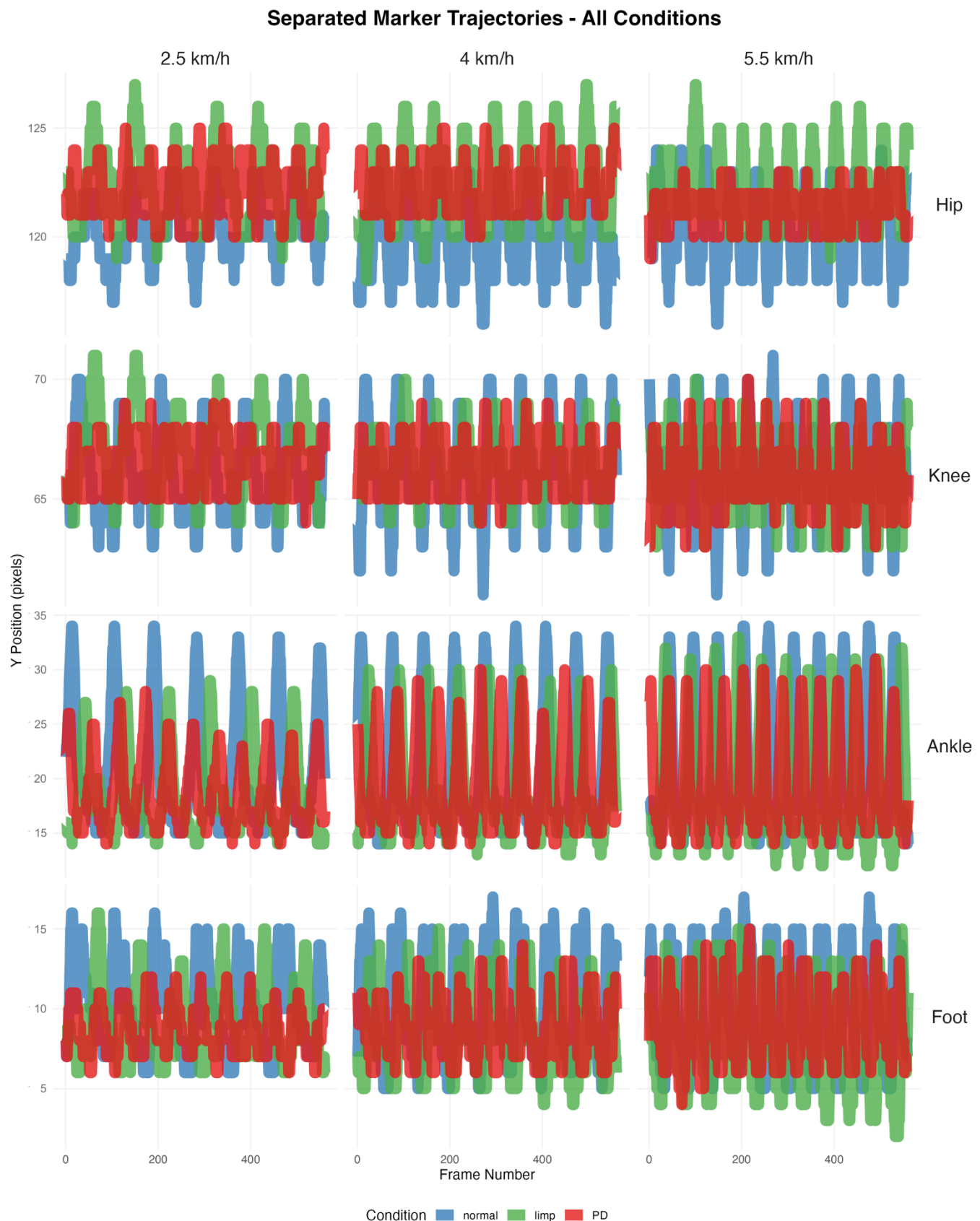
Appendix Figure 7. Marker Trajectory, Subject 3. All four markers plotted together, with direct comparison of normal, limping and Parkinsonian gait across 2.5, 4, and 5.5 km/h.



Appendix Figure 8. Marker Trajectory, Subject 3. All four markers plotted separately to enhance interpretability, with direct comparison of normal, limping and Parkinsonian gait across 2.5, 4, and 5.5 km/h. Marginal changes in baseline Y position of markers between or within speeds over time a result of slight camera tilt produced between recordings.

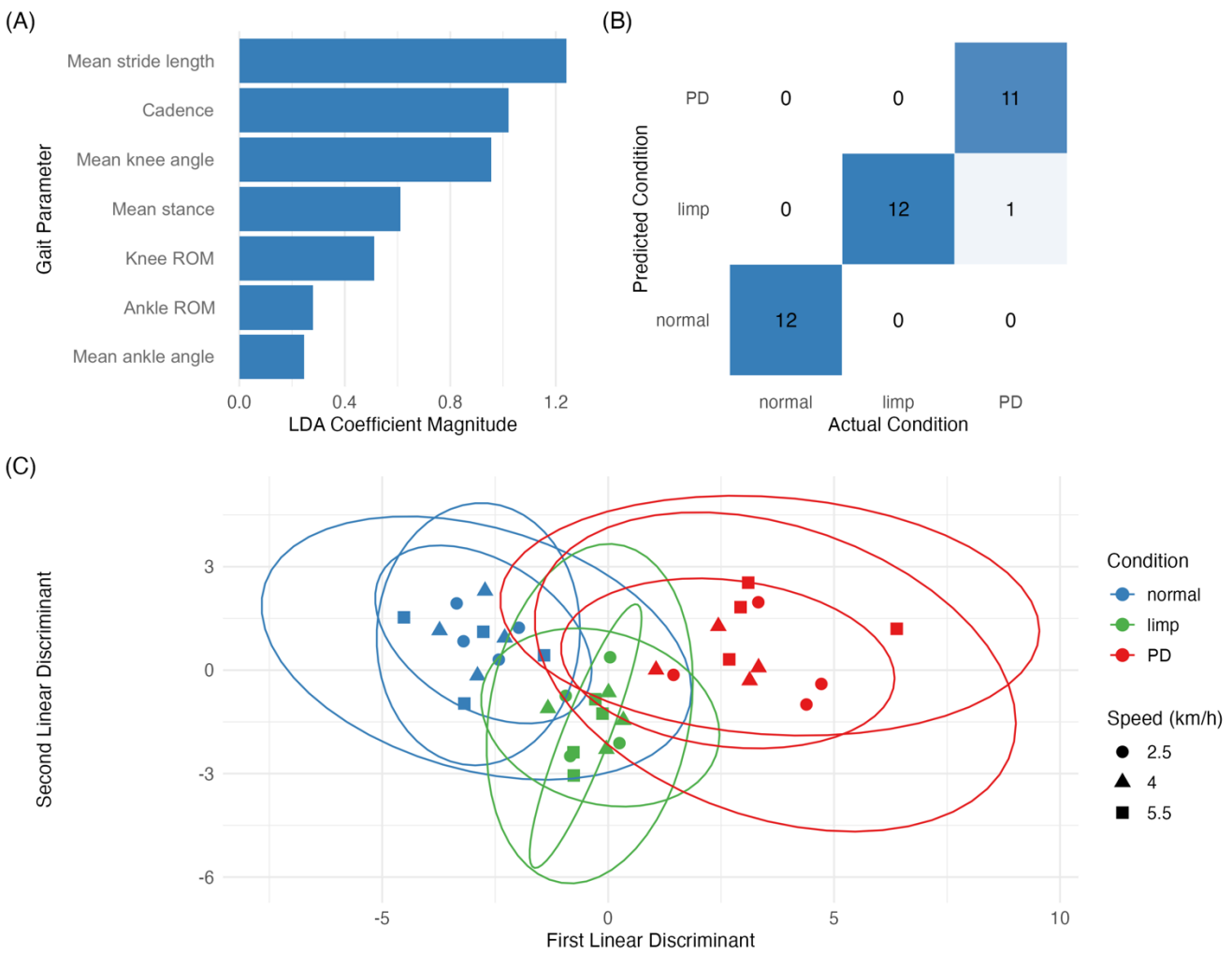


Appendix Figure 9. Marker Trajectory, Subject 4. All four markers plotted together, with direct comparison of normal, limping and Parkinsonian gait across 2.5, 4, and 5.5 km/h.



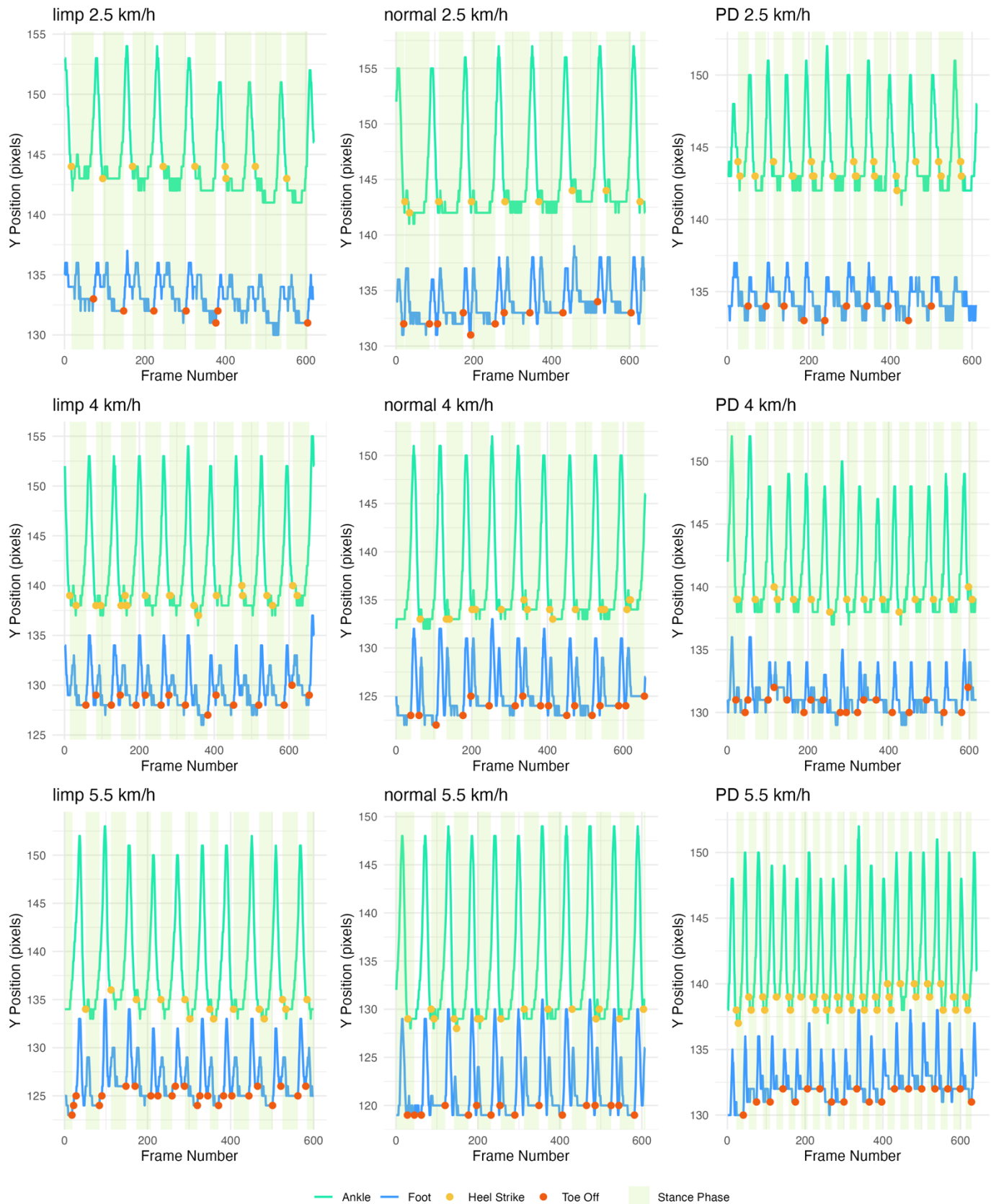
Appendix Figure 10. Marker Trajectory, Subject 4. All four markers plotted separately to enhance interpretability, with direct comparison of normal, limping and Parkinsonian gait across 2.5, 4, and 5.5 km/h. Marginal changes in baseline Y position of markers between or within speeds over time a result of slight camera tilt produced between recordings.

Gait Classification Analysis Using LDA



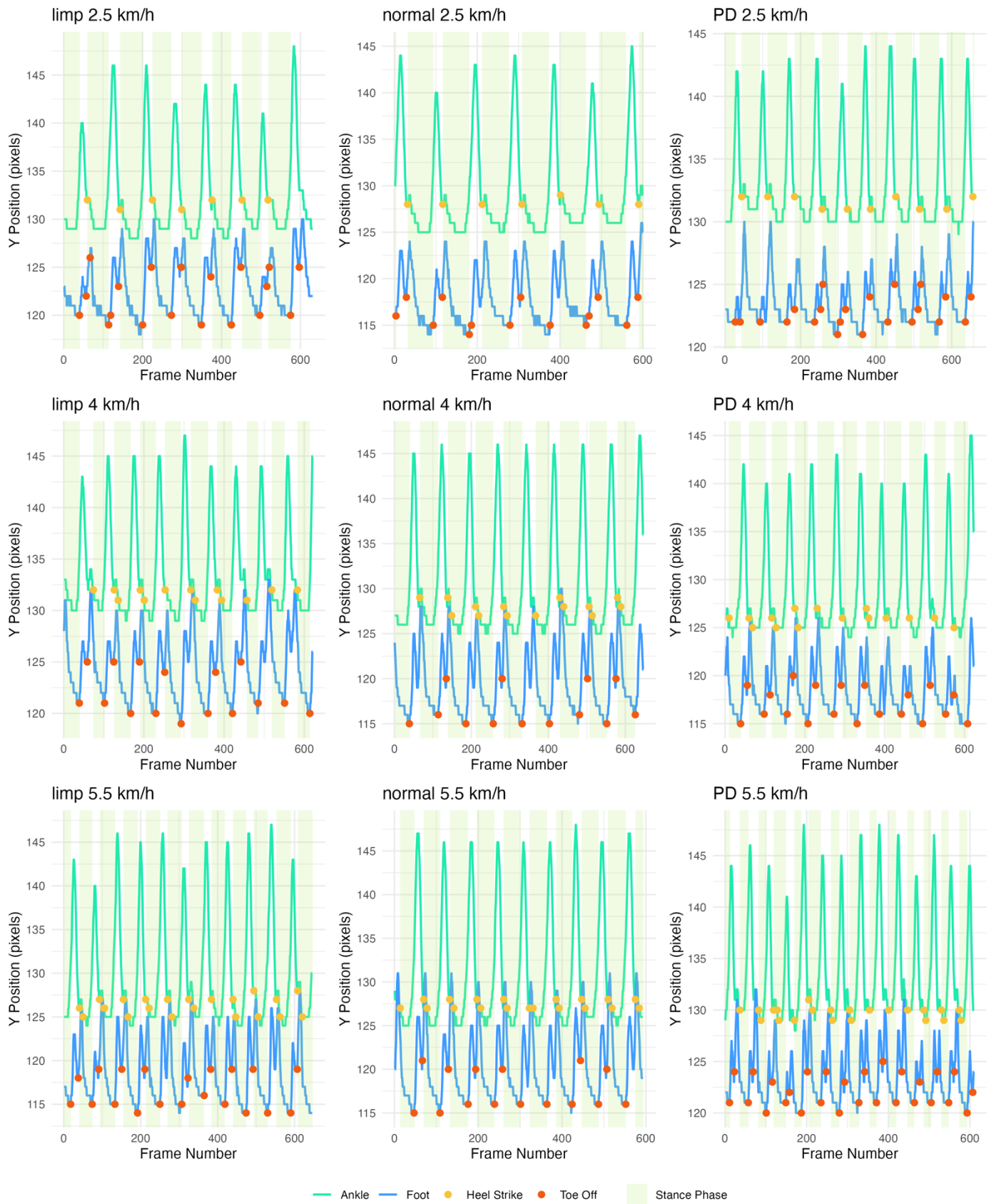
Appendix Figure 11. Gait Classification Analysis Using Linear Discriminant Analysis (LDA). (A) Relative importance of gait parameters in distinguishing between conditions, shown by LDA coefficient magnitude. Mean stride length and cadence emerged as the strongest discriminative features. (B) Confusion matrix showing classification performance across conditions. Each cell shows the number of cases, with darker blue indicating higher counts. (C) Scatter plot of the first two linear discriminants showing separation between gait conditions at different speeds, with 95% ellipses showing distribution of each condition.

Stance Phase Analysis: All Speeds and Conditions



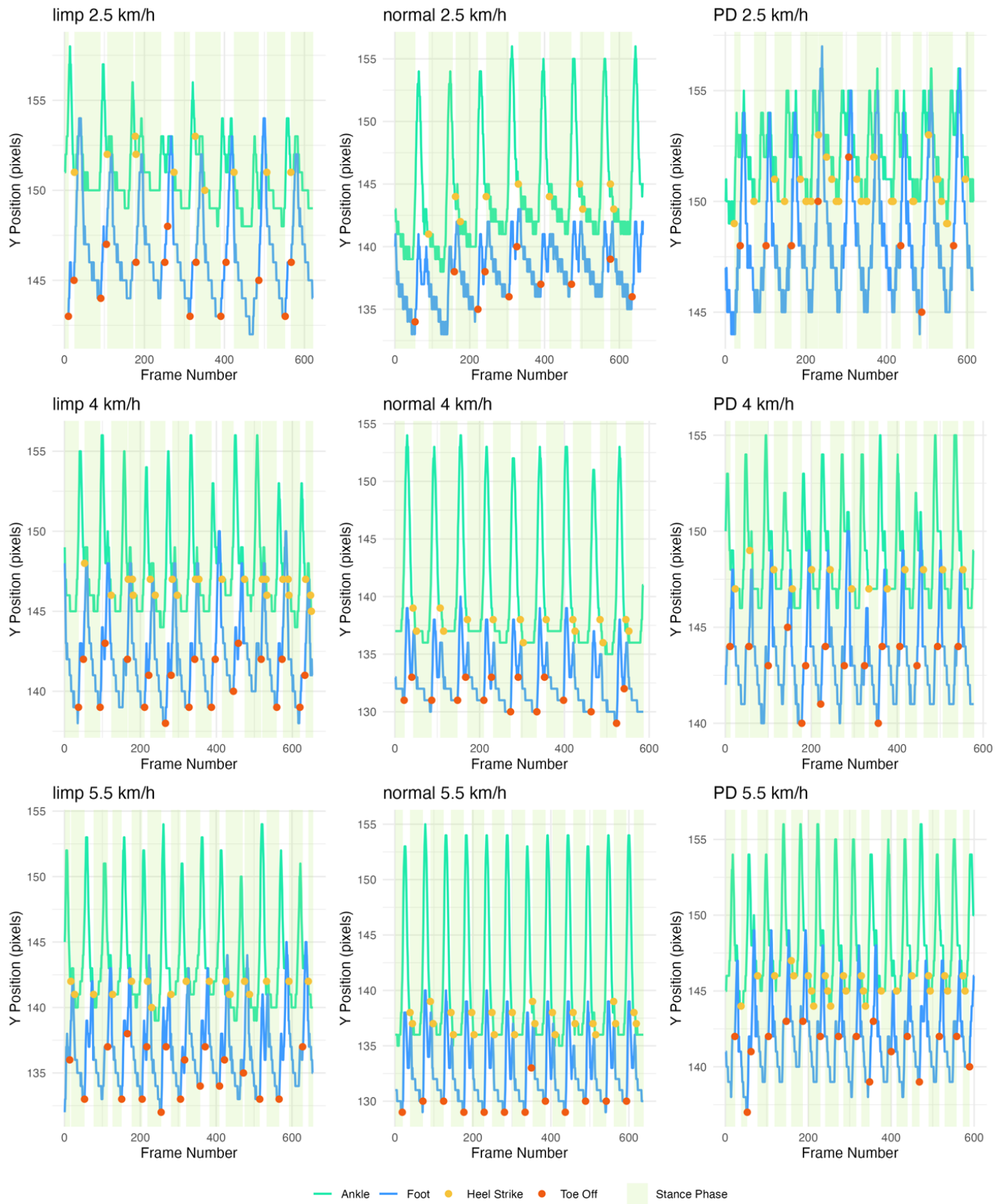
Appendix Figure 12. Stance Phase Analysis, Subject 1. Speed dependent thresholds were implemented for false heel strike (HS) and toe-off (TO) detection, to prevent false event detection impacting true stance phase.

Stance Phase Analysis: All Speeds and Conditions



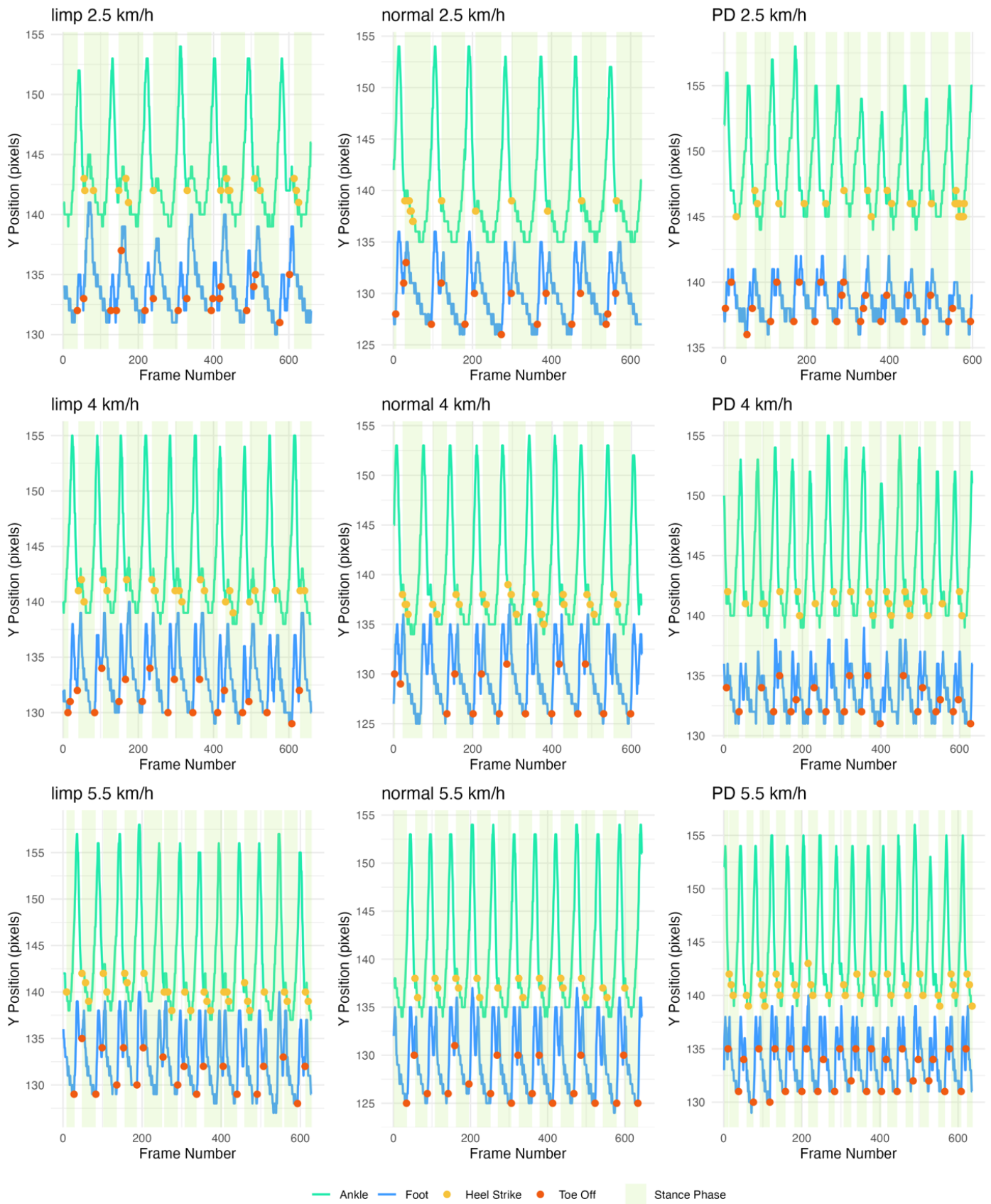
Appendix Figure 13. Stance Phase Analysis, Subject 2. Speed dependent thresholds were implemented for false heel strike (HS) and toe-off (TO) detection, to prevent false event detection impacting true stance phase.

Stance Phase Analysis: All Speeds and Conditions



Appendix Figure 14. Stance Phase Analysis, Subject 3. Speed dependent thresholds were implemented for false heel strike (HS) and toe-off (TO) detection, to prevent false event detection impacting true stance phase.

Stance Phase Analysis: All Speeds and Conditions



Appendix Figure 15. Stance Phase Analysis, Subject 4. Speed dependent thresholds were implemented for false heel strike (HS) and toe-off (TO) detection, to prevent false event detection impacting true stance phase.